

AD-A032 371

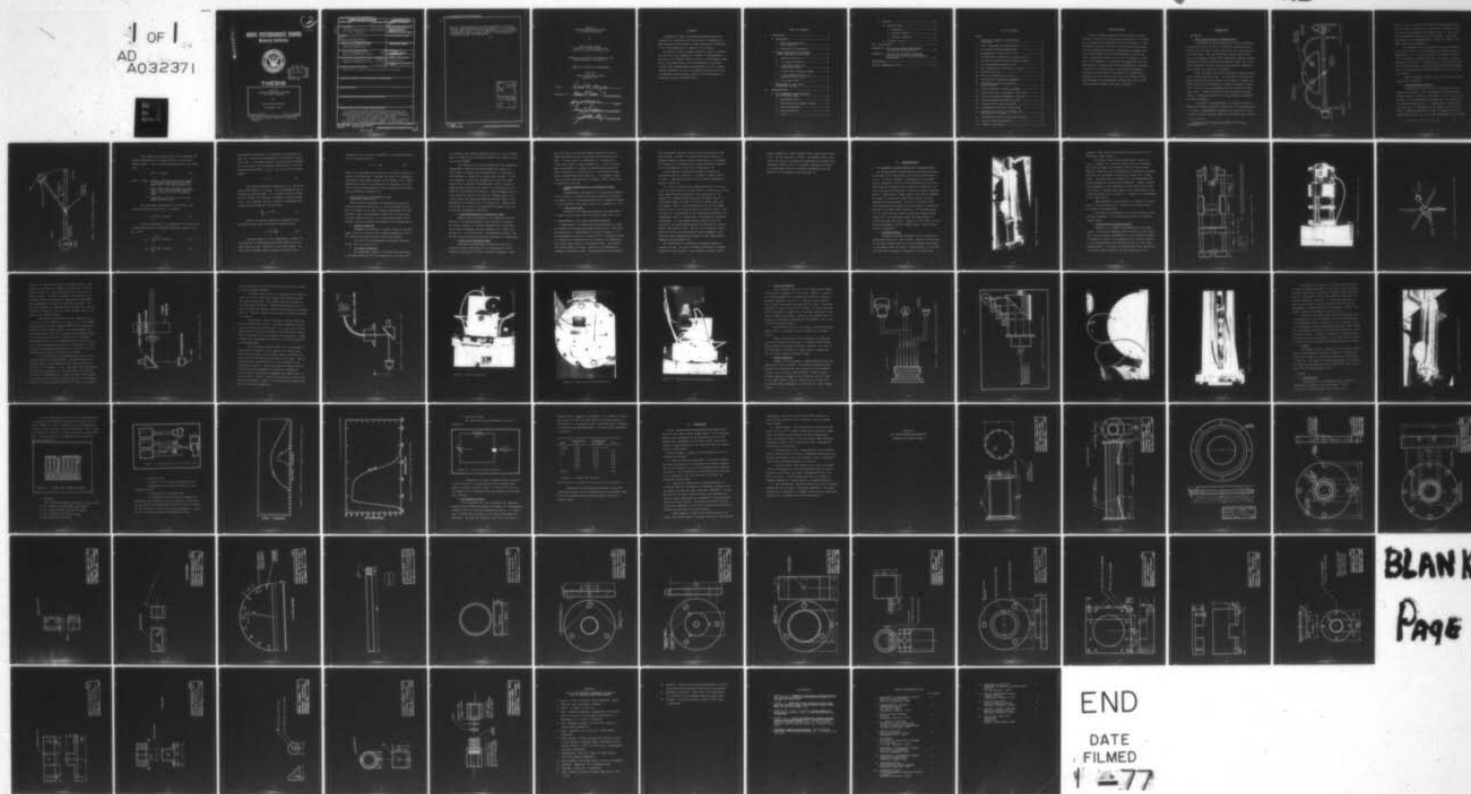
NAVAL POSTGRADUATE SCHOOL MONTEREY CALIF  
OPTICAL TRANSMISSOMETER-NEPHELOMETER FOR DEEP OCEAN USE.(U)  
SEP 76 D M MOSEY

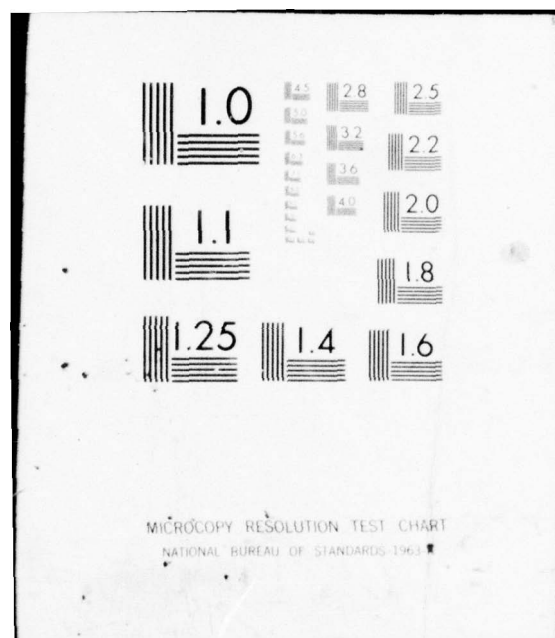
F/G 20/6

UNCLASSIFIED

NL

1 OF 1  
AD  
A032371



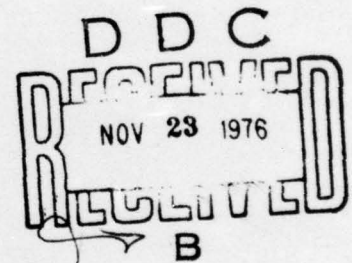


AD A032371

(2)  
NH

# NAVAL POSTGRADUATE SCHOOL

Monterey, California



## THESIS

OPTICAL  
TRANSMISSOMETER-NEPHELOMETER  
FOR DEEP OCEAN USE

by

David Michael Mosey

September 1976

Thesis Advisor:

S. P. Tucker

Approved for public release; distribution  
unlimited.

REPORT DOCUMENTATION PAGE		READ INSTRUCTIONS BEFORE COMPLETING FORM
1. REPORT NUMBER	2. GOVT ACCESSION NO.	3. RECIPIENT'S CATALOG NUMBER
4. TITLE (and Subtitle)		5. TYPE OF REPORT & PERIOD COVERED
(6) Optical Transmissometer-Nephelometer for Deep Ocean Use.		Master's Thesis, September 1976
7. AUTHOR(s)		6. PERFORMING ORG. REPORT NUMBER
(10) David Michael Mosey		8. CONTRACT OR GRANT NUMBER(s)
9. PERFORMING ORGANIZATION NAME AND ADDRESS		10. PROGRAM ELEMENT, PROJECT, TASK AREA & WORK UNIT NUMBERS
Naval Postgraduate School Monterey, California		
11. CONTROLLING OFFICE NAME AND ADDRESS		12. REPORT DATE
Naval Postgraduate School Monterey, California 93940		September 1976
14. MONITORING AGENCY NAME & ADDRESS (if different from Controlling Office)		13. NUMBER OF PAGES
Naval Postgraduate School Monterey, California 93940		76
		15. SECURITY CLASS. (of this report)
		Unclassified
		16a. DECLASSIFICATION/DOWNGRADING SCHEDULE
16. DISTRIBUTION STATEMENT (of this Report)		
Approved for public release; distribution unlimited.		
17. DISTRIBUTION STATEMENT (of the abstract entered in Block 20, if different from Report)		
18. SUPPLEMENTARY NOTES		
19. KEY WORDS (Continue on reverse side if necessary and identify by block number)		
20. ABSTRACT (Continue on reverse side if necessary and identify by block number)		
<p>A submersible light transmissometer-nephelometer was designed and constructed for the purpose of measuring the beam attenuation and relative volume scattering coefficients at two fixed angles and at depths to 1000 meters.</p> <p>Flexibility, a major design criterion, makes it possible for the unit to be operated in a number of configurations. Addition of an internal battery supply, a filter wheel, light</p>		

251450

over  
PB



stops, a photomultiplier tube and amplifiers is possible. The NPS light transmissometer-nephelometer is not a single purpose instrument but has the capability to be utilized as a submersible optical bench, useful in the development of underwater optical instrumentation.

ACCESSION for	
NTIS	White Section <input checked="" type="checkbox"/>
DDC	Buff Section <input type="checkbox"/>
UNANNOUNCED	<input type="checkbox"/>
JUSTIFICATION	
BY	
DISTRIBUTION/AVAILABILITY CODES	
Dist.	AVAIL. and/or SPECIAL
A	

DD Form 1473  
1 Jan 73  
S/N 0102-014-6601

Optical  
Transmissometer-Nephelometer  
for Deep Ocean Use

by

David Michael Mosey  
Lieutenant, United States Navy  
B.S.E.E., Purdue University, 1971

Submitted in partial fulfillment of the  
requirements for the degree of

MASTER OF SCIENCE IN OCEANOGRAPHY

from the  
NAVAL POSTGRADUATE SCHOOL  
September 1976

Author

*David M. Mosey*

Approved by:

*Steven P. Tucker*

Thesis Advisor

*John H. Kahlbach*

Reader

*Dale F. Lipper*

Chairman, Department of Oceanography

*John B. Bunting*

Academic Dean

# ABSTRACT

A submersible light transmissometer-nephelometer was designed and constructed for the purpose of measuring the beam attenuation and relative volume scattering coefficients at two fixed angles and at depths to 1000 meters.

Flexibility, a major design criterion, makes it possible for the unit to be operated in a number of configurations. Addition of an internal battery supply, a filter wheel, light stops, a photomultiplier tube and amplifiers is possible. The NPS light transmissometer-nephelometer is not a single purpose instrument but has the capability to be utilized as a submersible optical bench, useful in the development of underwater optical instrumentation.



## TABLE OF CONTENTS

I.	INTRODUCTION - - - - -	9
A.	BACKGROUND - - - - -	9
	1. Water Characteristics Instrumentation - - - - -	9
	2. Scattering and Absorption - - - - -	11
B.	OTHER TECHNIQUES FOR MEASURING VOLUME ATTENUATION COEFFICIENT - - - - -	15
	1. Contrast Reduction - - - - -	15
	2. c at High Collimation - - - - -	15
	3. c from Measurements of Irradiance on Axis - - - - -	16
	4. c from Visual Threshold Range - - - - -	16
	5. c from Telephotometry of an Extended Diffuse Source - - - - -	17
	6. c for Laser Light - - - - -	17
C.	MEASUREMENT OF THE VOLUME SCATTERING FUNCTION - - - - -	17
II.	INSTRUMENTATION - - - - -	20
A.	NPS UNDERWATER TRANSMISSOMETER AND SCATTERING METER - - - - -	20
	1. Collimated Source - - - - -	20
	2. Receiver/Optical Sampler Section - - - - -	22
	3. Power Requirements - - - - -	33
	4. System Operation - - - - -	33
	5. Output - - - - -	38

B. RESULTS	38
1. Bench Testing	38
a. Equipment	40
b. Optical Filters	41
c. Detector Biasing	44
2. In-Water Testing	44
III. CONCLUSIONS	46
APPENDIX A: NPS Transmissometer-Nephelometer Drawings and Specifications	48
APPENDIX B: List of Off-the-Shelf Components Utilized in the NPS Transmissometer- Nephelometer	72
BIBLIOGRAPHY	74
INITIAL DISTRIBUTION LIST	75



## LIST OF FIGURES

### Figure

1.	Simplified diagram of dual purpose instrument - - - - -	10
2.	Basic nephelometer configuration - - - - -	12
3.	NPS Transmissometer-Nephelometer - - - - -	21
4.	Arrangement of components on rods - - - - -	23
5.	Transmissometer-nephelometer light source - - - - -	24
6.	Schematic representation of detector inputs - - - - -	25
7.	Ray diagram-mirror position one - - - - -	27
8.	Ray diagram-mirror positions 2, 3 and 4 - - - - -	29
9.	Detector mounting - - - - -	30
10.	Mirror positioning drive motor - - - - -	31
11.	Photodetector mounting arrangement - - - - -	32
12.	Underwater electrical connector wiring diagram - - - - -	34
13.	System operation conceptual diagram - - - - -	35
14.	Scattering sensor arrangement, side view - - - - -	36
15.	Scattering sensor arrangement, top view - - - - -	37
16.	Transmissometer-nephelometer system - - - - -	39
17.	Voltage output, bench operation - - - - -	40
18.	Experimental set-up for bench tests - - - - -	41
19.	Transmission curves for Corning 1-57 and Wratten 61 filters - - - - -	42
20.	Transmission curve for Hoya HA-30 filter - - - - -	43
21.	Detector biasing schematic - - - - -	44
22.	In-water test results - - - - -	45

## ACKNOWLEDGEMENT

I wish to express appreciation to my thesis advisor, Stevens P. Tucker for his interest and patience in overseeing the design and construction of the instrument; to the NPS Machine Facility for their cooperation in fabricating the many components required; to Machinery Repairman First Class Travis Adams for his professionalism in machining several components under a severe time constraint; to Prof. (Ret.) Sid Kalmbach of the NPS Physics Department for his professional evaluation and advice concerning the finished product; to the technicians of the Physics Department, especially Bob Moeller and Tom Maris, who supplied many components for the device; and to my wife Kathryn for her understanding and encouragement during times when my work necessitated my absence from home and family.

## I. INTRODUCTION

### A. BACKGROUND

#### 1. Water Characteristics Instrumentation

A knowledge of certain underwater optical parameters is essential if one wishes to characterize optically a particular type of water in which operations involving light are to be conducted. Such operations may include among others the use of imaging systems, fixed underwater lighting, remote underwater television cameras and external lights for use on deep submergence vehicles, optical detection and communication systems, and near-shore bathymetry.

Many instruments have been developed to measure underwater optical characteristics. The instrument which was designed and constructed was made in an attempt to combine two meters into one for measuring the volume attenuation coefficient  $c(\lambda)^*$  at visual wavelengths and the scattering coefficient,  $\beta(\theta)$ . These quantities will be discussed in detail later. A simplified diagram of the dual-purpose instrument is shown in Figure 1.

In general a transmissometer or c-meter is used to measure the volume attenuation coefficient at some wavelength,  $\lambda$ . A basic transmissometer consists of a light source with a narrow, highly collimated beam and a receiver with a narrow

---

\*Frequently this attenuation coefficient has been designated by " $\alpha$ ".



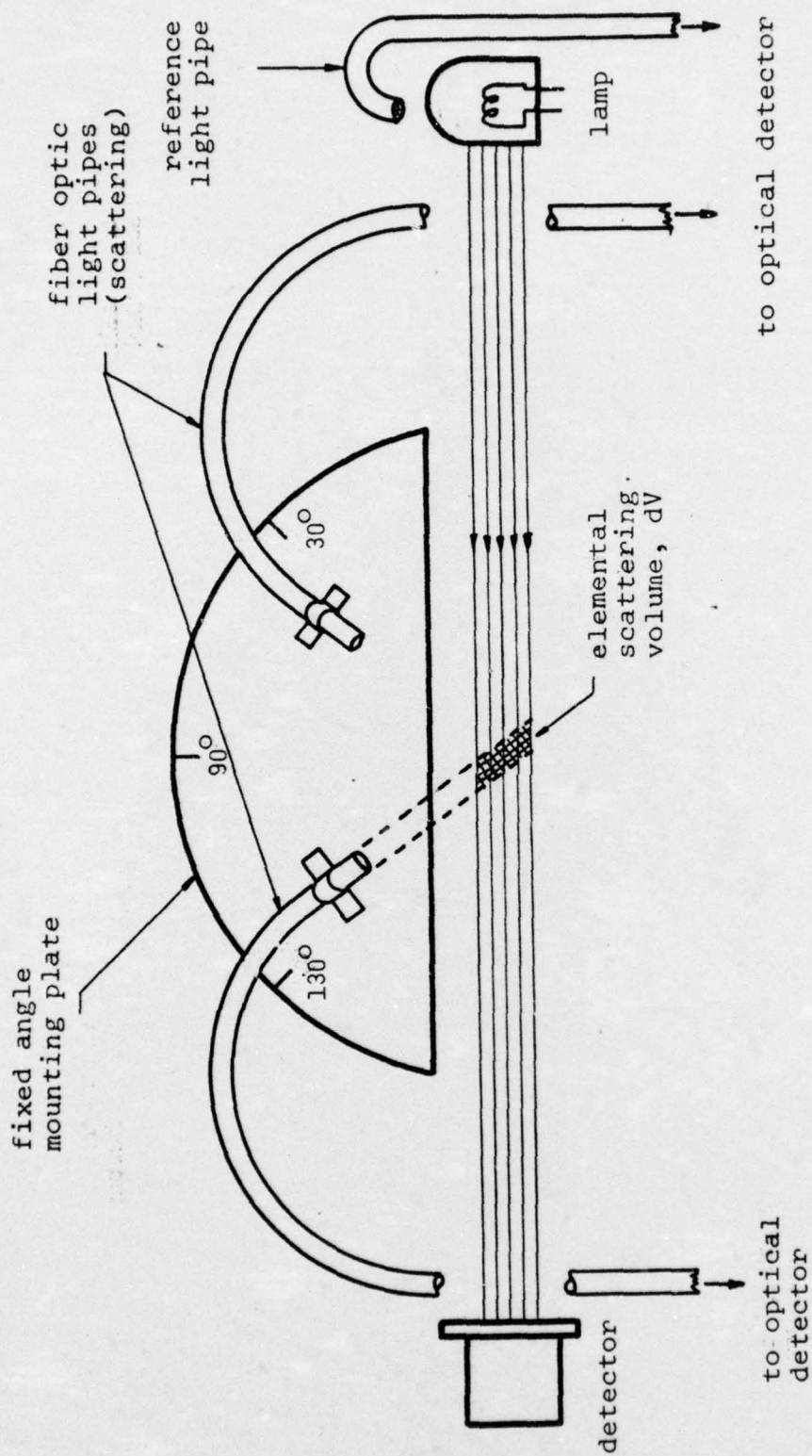


Figure 1. Simplified diagram of dual purpose instrument.

field of view. The source and detector are separated by a fixed distance, usually one to two meters. Normally, photocells are used to measure the radiant output of the source and the irradiance detected at the receiver. From these measurements, the transmissivity,  $T$ , over the length of the beam's path can be determined.

An instrument used to determine the volume scattering function,  $\beta(\theta)$ , is the large-angle scattering meter or nephelometer [5]. In this instrument the light scattered from an elemental scattering volume is recorded by a photodetector that rotates in a semicircle at a fixed radius from the scattering volume,  $\theta$  being the angle between the optical axis of the detector and the forward direction of the source (see Figure 2).

These instruments measure two of the inherent optical properties of seawater.

## 2. Scattering and Absorption

Attenuation of light is due to the effects of scattering and absorption. The attenuation of a beam passing through seawater can thus be considered to be the sum of the effects of (1) scattering by the water,  $b_w$ ; (2) scattering by dissolved material,  $b_d$ ; (3) scattering by suspended particulates,  $b_p$ ; (4) absorption by the water,  $a_w$ ; (5) absorption by dissolved material,  $a_d$ ; and (6) absorption by suspended particulates,  $a_p$ . It is then described by the relation

$$c = a_w + a_d + a_p + b_w + b_d + b_p \quad (1)$$



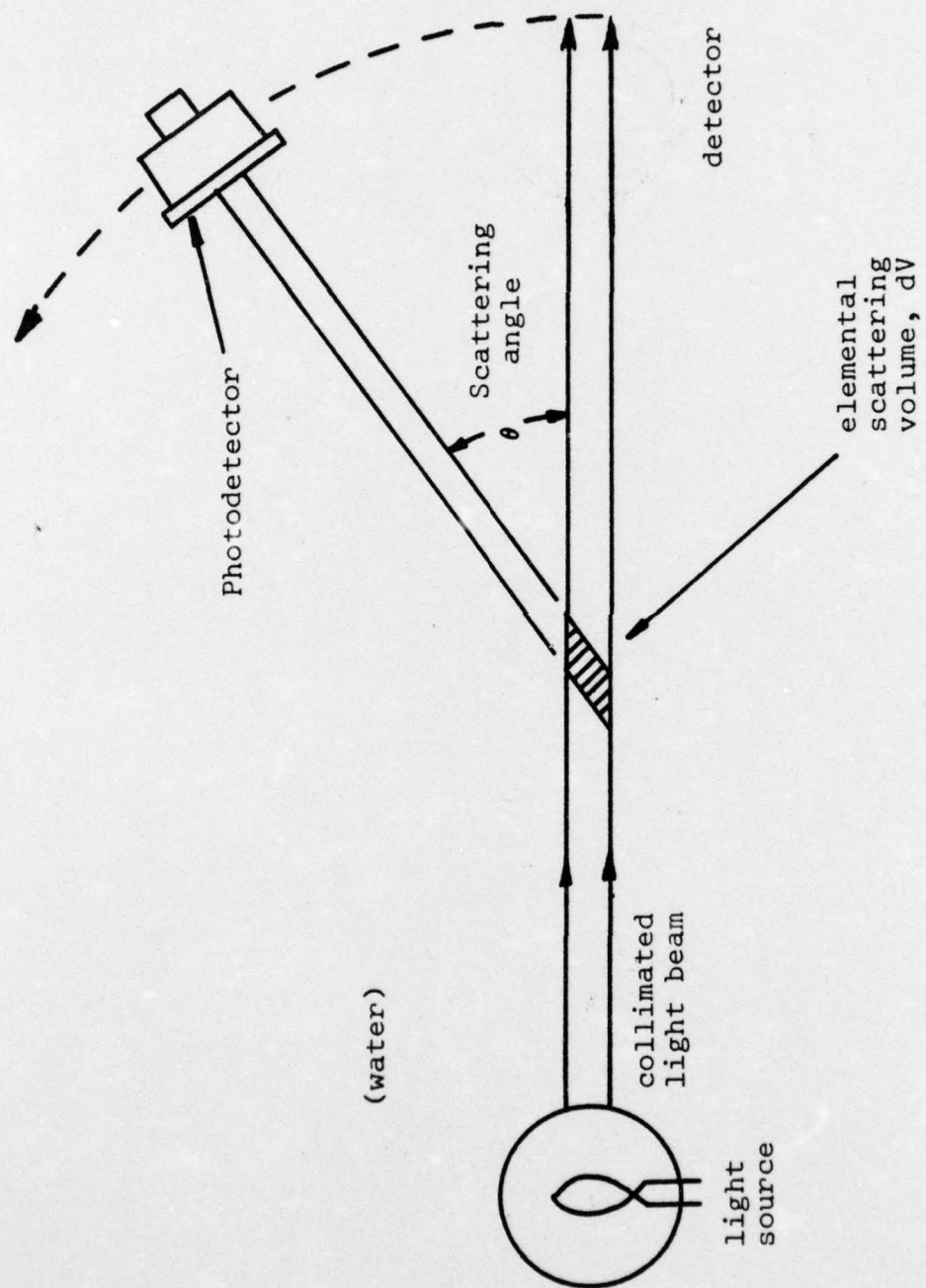


Figure 2. Basic nephelometer configuration.

The volume scattering function,  $\beta(\theta)$  describes the angular dependence of the light scattered from a small volume element.  $\beta(\theta)$  is defined operationally by the equation:

$$dJ(\theta) = \beta(\theta)HdV \quad (2)$$

where  $dJ(\theta)$  = radiant intensity (power/solid angle) of the light scattered from a collimated beam in the volume element  $dV$ .

$\theta$  = polar angle which describes the direction of the scattered light with respect to the axis of the collimated beam.

$H$  = irradiance (power/unit area) of the light incident on  $dV$ .

The scattering coefficient  $b$ , is related to the volume scattering function  $\beta(\theta)$  as follows:

$$b = 2\pi \int_0^\pi \beta(\theta) \sin\theta \, d\theta \quad (3)$$

$b$  may be considered to be composed of a forward scattering term,  $b_f$ , and a backscatter term,  $b_b$ , where  $b = b_f + b_b$ . Thus:

$$b_f = 2\pi \int_0^{\pi/2} \beta(\theta) \sin\theta \, d\theta \quad (4)$$

$$b_b = 2\pi \int_{\pi/2}^\pi \beta(\theta) \sin\theta \, d\theta \quad (5)$$

An absorption coefficient  $a$ , describes the attenuation of light for a particular wavelength by the absorption mechanism alone. It strongly depends on the optical wavelength, and is related to the attenuation coefficient,  $c$ , and the scattering coefficient,  $b = b_w + b_d + b_p$ , in the following manner:

$$a = c - b \quad (6)$$

The volume attenuation coefficient  $c(\lambda)$ , can be defined operationally as follows: if a collimated source of radiance  $N_0$  and wavelength  $\lambda$  is directed through a medium (such as water), the radiance at distance  $r$  down the beam is  $N_r$ .  $N_r$  is smaller than  $N_0$  - because of absorption and scattering in the medium - by the ratio:

$$\frac{N_r}{N_0} = e^{-c(\lambda)r} \quad (7)$$

Hence, the volume attenuation coefficient for a collimated light source described is defined as [2]:

$$c = -\frac{1}{r} \ln \frac{N_r}{N_0} \quad (8)$$

The measurement of  $c$  is, complicated, however, by the necessity to distinguish unscattered light from the light which has been scattered at very small angles. Because some scattered light is always collected at the



receiver of even the best instruments, the measured attenuation is actually given by:

$$c' = c + gb \quad (9)$$

where  $g$  is some number less than one, the value of which depends on the instrument. Because the value of the measured attenuation coefficient depends on the design of the instrumentation as well as the properties of the water, the accuracy of reported measurements of the attenuation coefficient must be carefully evaluated [5].

#### B. OTHER TECHNIQUES FOR MEASURING VOLUME ATTENUATION COEFFICIENT

There are many techniques for measuring the spectral volume attenuation coefficient,  $c$ , and no attempt will be made to present all of them. Several significant and quite different types of measurements, which in all cases yield the same numerical result, will be mentioned briefly here. Duntley [1] gives detailed discussions of such measurements.

##### 1. Contrast Reduction

Underwater photographs of objects taken in the horizontal direction disclose that a simple exponential form of the contrast reduction equation holds for daylight.

The value of the attenuation coefficient measured in this way is in fact  $c$  [3].

##### 2. $c$ at High Collimation

By varying the length of the water path and making a semilogarithmic plot of flux received vs. distance from

a collimated light source, absolute values of  $c$  can be found from the slope of the resulting straight line without requiring an air reading.

The values of attenuation coefficient are remarkably unaffected by beam and receiver geometry as long as (1) stray light is effectively eliminated and (2) the ratio of beam diameter to length of the water path is small. It is not necessary to have high collimation at both the light source and the receiver, although stray light is easier to suppress when some practical amount of collimation is provided for both source and receiver. Beam divergence and receiver field of view of the order of 1 degree seems to be a good choice for fixed path transmissometers using an air measurement to establish the  $c=0$  reading [1]. Higher collimation does not result in an appreciably different value of the volume attenuation coefficient.

### 3. $c$ from Measurements of Irradiance on Axis

Several ways of measuring  $c$  are suggested when the receiver of a transmissometer is an irradiance collector. The curves obtained for various combinations of beam diameters, beam divergences and path segments will follow the  $c$ -slope [3]. In most practical circumstances, however, they are not attractive options from the standpoint of convenience.

### 4. $c$ from Visual Threshold Range

Underwater psychophysical experiments show that laboratory visual threshold data are applicable to valid numerical predictions of visual threshold distances. Such



data show that black-suited swimmers having no areas of higher reflectance will, when deployed horizontally, lose sight of each other at a separation of 4 attenuation lengths when there is ample daylight [3]. Thus, two swimmers can determine  $1/c$  simply by separating horizontally while connected by a measuring line. One fourth of their mutual disappearance range equals  $1/c$ . No equipment other than a knotted, measured line is needed. Water clarity may be measured in this way.

5. c from Telephotometry of an Extended, Diffuse Source

Telephotometer measurements of the apparent radiance of the center of a diffusely emitting surface will produce a straight line on a semilogarithmic plot of apparent radiance vs. lamp distance, the slope of which is a measure of  $c$  [3].

6. c for Laser Light

Several of the foregoing techniques are applicable to laser sources, which lead to the same values for  $c$  [3].

C. MEASUREMENT OF THE VOLUME SCATTERING FUNCTION

A nephelometer, or large angle scattering meter is used to determine the volume scattering function  $\beta(\theta)$ . The basic configuration of a nephelometer is shown in Figure 2. In the measurement of  $\beta(\theta)$  as a function of  $\theta$ , scattering volume is recorded by a photodetector that rotates in a semicircle at a fixed radius from the scattering volume. One problem with nephelometers has been a difficulty in defining the elemental scattering volume. Another problem occurs because

the instruments normally cannot measure scattering at very small angles. Because the volume scattering function is strongly peaked at small angles, errors occur in attempting to evaluate  $b$  by integrating the volume scattering function that is determined by this type of instrument. [5].

If the complete scattering function is desired the scatterance must be observed at a number of angles from  $0^\circ$  to  $180^\circ$ . A general discussion of the various techniques is given by Jerlov [3].

If  $b$  is to be obtained the observations must cover both small and large angles, and they should be carried out in situ. Small angle forward scattering is due especially to the presence of suspended particles which in number lead to a significant amount of light scattered at angles less than one degree. Most in vitro measurements are in the angular interval  $10^\circ$  to  $165^\circ$  and given only in relative units. This prevents (1) a calculation of the scattering coefficients by integration, and (2) a separation of molecular and particle scatterance. In the present review, attention has been focused on the observations giving absolute values, and primarily those made in situ. The in vitro technique is hampered by the risk of contamination and of changes in the particles while sampling and during the time lapse between sampling and measurement [3].

The calibration of scattering instruments presents a special problem. The use of standard scatterers or perfect diffusers is not reliable. The technique of Morel (1966)

using benzene as a known standard gives very accurate relative - but not absolute - results. Kullenberg (1968, 1969) avoids the use of a reference by measuring the intensity and elemental volume. This is a reliable technique, provided the scattering volume is accurately determined, and the geometry of the system is well defined [3].



## II. INSTRUMENTATION

### A. NPS UNDERWATER TRANSMISSOMETER AND SCATTERING METER

The NPS Underwater Transmissometer and Scattering meter was designed and constructed by the author and Stevens P. Tucker. It was an attempt to incorporate off-the-shelf optical components and solid state photodetection devices. The mechanical complexity was minimized by using only one motor with associated gearing to drive the optical sampling mirror. Fiber-optics ("light pipes") were used to minimize the number of prisms and lenses which require critical alignment and positioning. The use of a single, solid-state photodetector provides an output which is always referenced to the same light intensity. The one-meter path for the light beam was chosen to keep the optical system simple and is an acceptable length for measurements in coastal and upwelling areas. Figure 3 is an overall view of the NPS instrument, and the numbers refer to part numbers listed in Appendix A.

#### 1. Collimated Source

Originally the NPS instrument was to incorporate a helium-neon laser as a light source. However, difficulties in the high voltage supply of the unit necessitated return to the manufacturer for repair. Unfortunately, the particular laser was no longer in production, and repair was

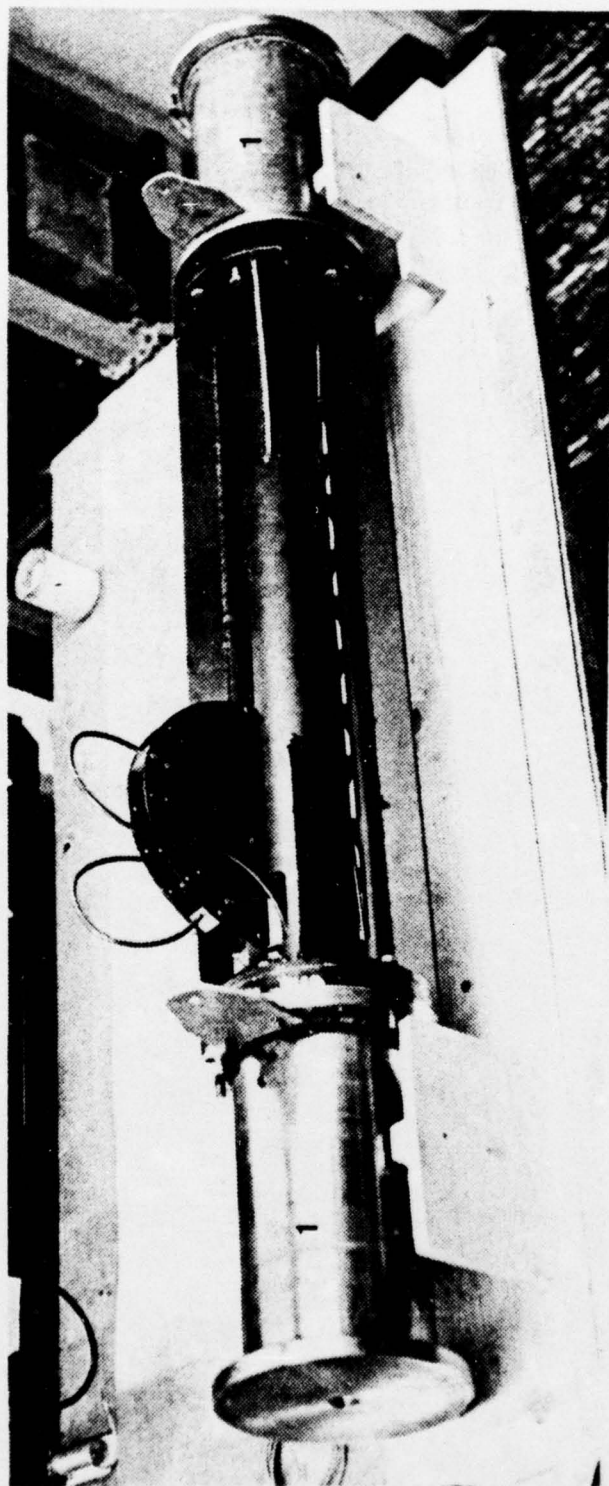


Figure 3. NPS Transmissometer-Nephelometer.



untimely. These facts necessitated the construction of an alternative light source.

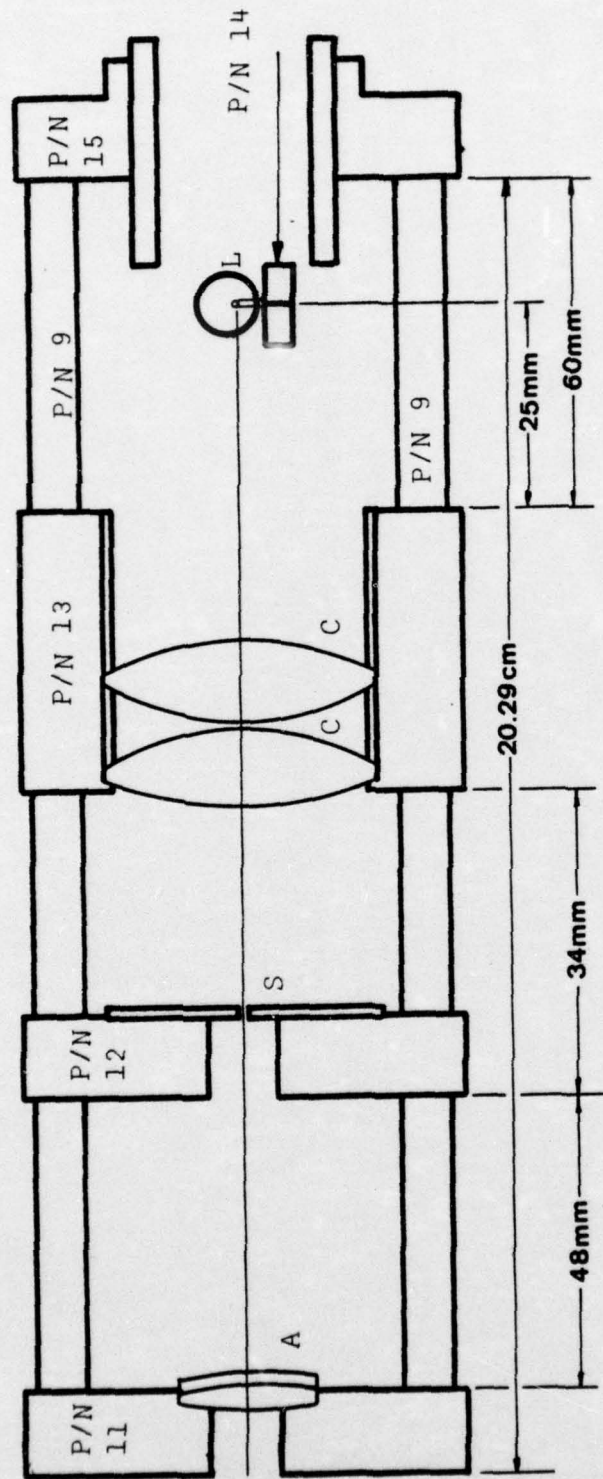
The quartz-iodine lamp adopted draws 3 amps at 6 volts to produce the intensity required for the instrument. Rays from the lamp are collected by back-to-back mounted aspheric condensers, and collimated by a two element achromat. They exit the instrument horizontally through the 1" pyrex window. Off-axis rays are limited by a .040" diameter stop placed between the achromat and condensers. Figure 4 depicts the arrangement of the components on the slider rods in sectional view. Provisions are made for the installation of an additional field stop in front of A. Figure 5 is a photograph of the light source.

Beam diameter at the receiver is 19 mm and its divergence is of the order of  $1^{\circ}$ . Duntley [3] has shown such a divergence to be acceptable.

The source is contained in one of two stainless steel pressure housings. It is bolted to one end of an aluminum support frame.

## 2. Receiver/Optical Sampler Section

Figure 6 is a schematic representation of detector inputs. The optical sampling system utilized in this instrument provides several advantages over other sampling methods. It enables all inputs to be sampled by one detector, whether it is a photodetector, photomultiplier tube or other light sensing device. All inputs are continually being referenced to the same light intensity, and any variation in this



A - achromatic objective lens

C - condensers

L - lamp

S - .040" stop

Note: Mounting component numbers are part numbers (P/N) found on drawings shown in Appendix A.

Figure 4. Arrangement of components on rods.

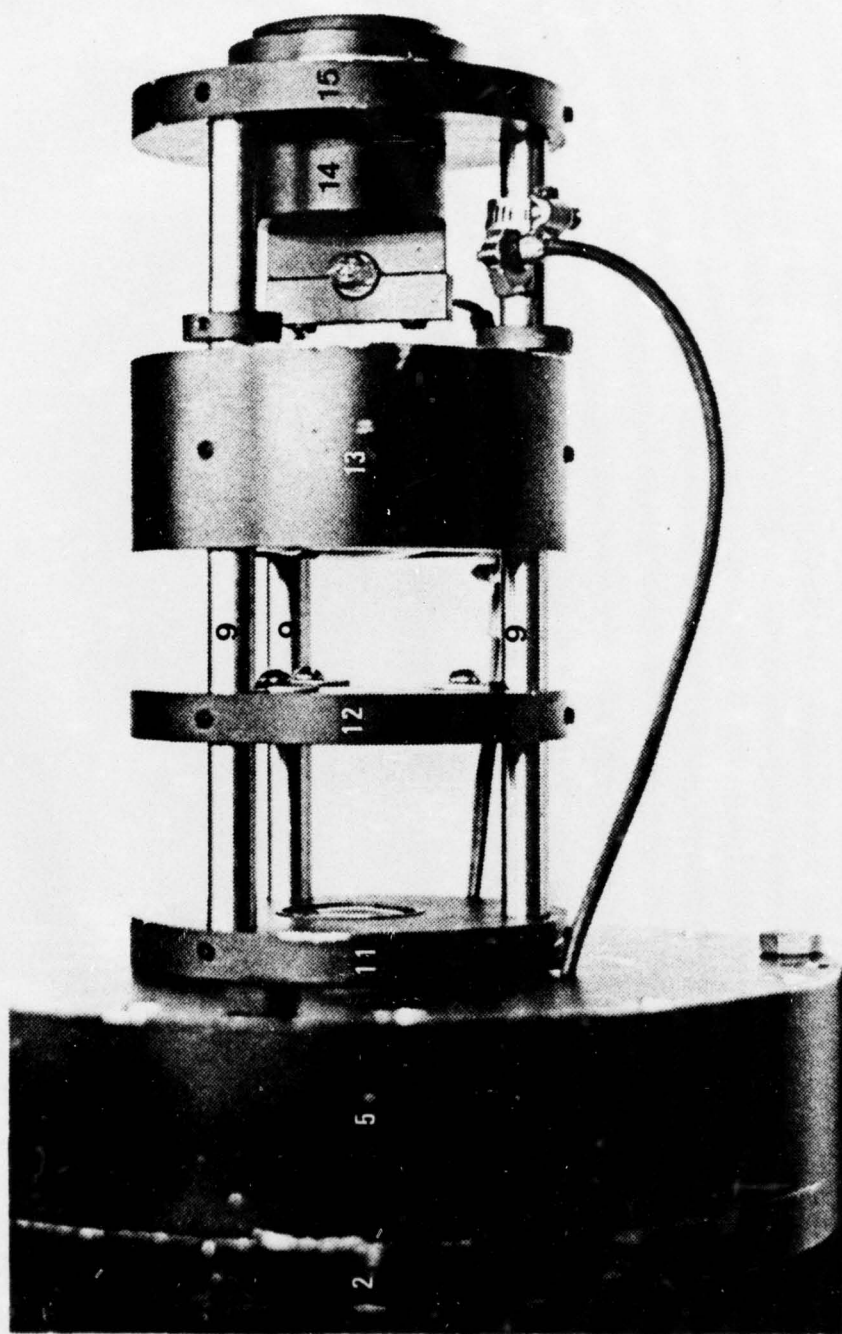


Figure 5. Transmissometer-nephelometer light source.



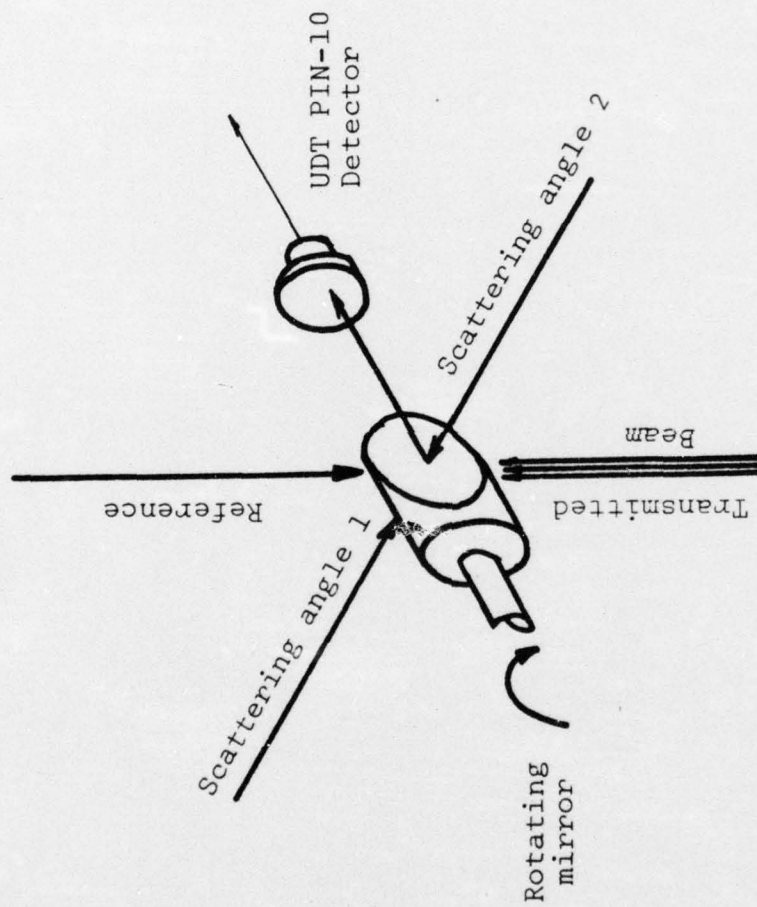


Figure 6. Schematic representation of detector inputs.

intensity is readily observed on the output record. Additionally, the sequential sampling of this type of system always includes the light reference level in each set of sampled values. Finally, the method is mechanically and optically simple and reliable as there are no complicated lens arrangements to direct and re-focus the beam. The motor that drives the sampling mirror requires only one set of gears, one gear on the motor shaft and the other on the shaft of the sampling mirror.

This method of sequential optical sampling is like that used in other samplers in current use [4]. The Defense Meteorological Satellite Program (DMSP) Block 5D satellite contains a sensor which samples in a similar manner [4]. A diagonal mirror driven by a stepper motor, samples humidity, temperature and ozone by making a set of radiance measurements which are then mathematically inverted to provide vertical compositional profiles. The degree of sophistication is necessarily greater than the NPS unit, but the principles and theory of operation are similar.

In the NPS meter the collimated light beam is projected through the seawater along a one-meter path and is incident upon a 55-mm achromatic lens, which focuses the rays down to a diameter of 3 mm. The light rays then reflect off the front surface of the rotating mirror (in position one) into the photodetector. Figure 7 depicts the ray path to the solid state detector in this position. As the mirror rotates it cycles through positions 2, 3, and 4 in sequence.

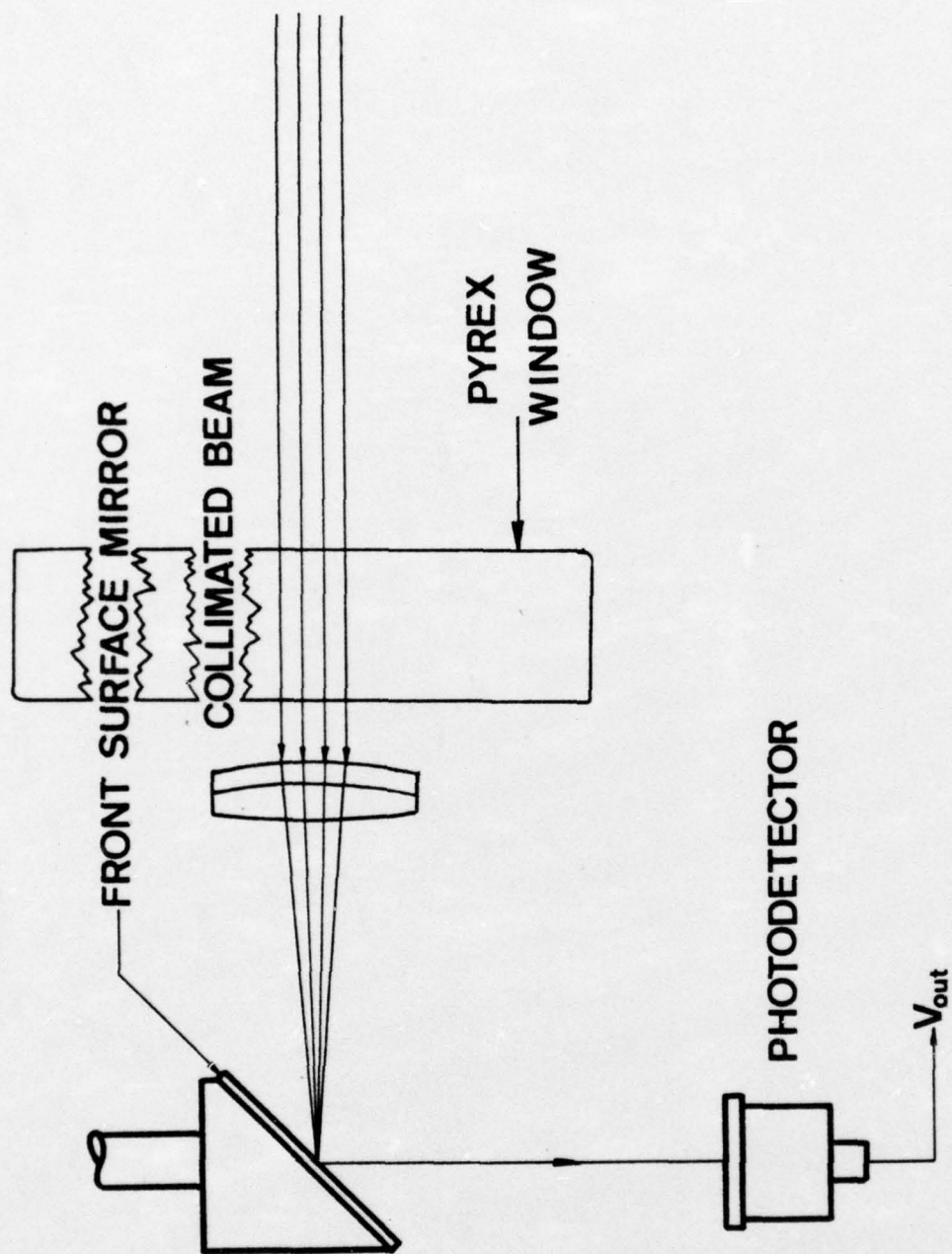


Figure 7. Ray diagram-mirror position one.



These positions and their functions are described in detail in the following paragraphs.

In mirror position two, the sampling mirror receives light rays from a fiber optic light pipe originating near the quartz-iodine bulb. The terminal end of this pipe is the fiber-optic end mount. These reflected rays are the means by which the reference intensity is sensed by the photodetector. Figure 8 depicts the ray paths in mirror positions 2, 3, and 4.

In positions 3 and 4 the mirror reflects light rays from the fiber-optic sensors. The only difference between these positions and position one is the origin of the input. Scattering of the beam is sensed by the fiber-optic bundles which are mounted on the fixed-angle mounting plate. Figure 1 depicts the approximate positions of the fiber bundles on the mounting plate.

The fixed-angle mounting plate has the advantage of being able to change the input angle to the light pipes. The fiber-optic mounts are drilled, tapped, and keyed with dowel pins to allow manual adjustment in  $20^\circ$  steps. The adjustment holes are positioned in an arc centered on the scattering volume dV. Thus, scattering for angles from  $10^\circ$  to  $170^\circ$  may be investigated with some minor adjustment. Figure 9 shows the detector arrangement and fiber optic input positions. Figure 10 depicts the mirror drive motor and associated gearing. Figure 11 illustrates the photodetector and its mounting configuration.

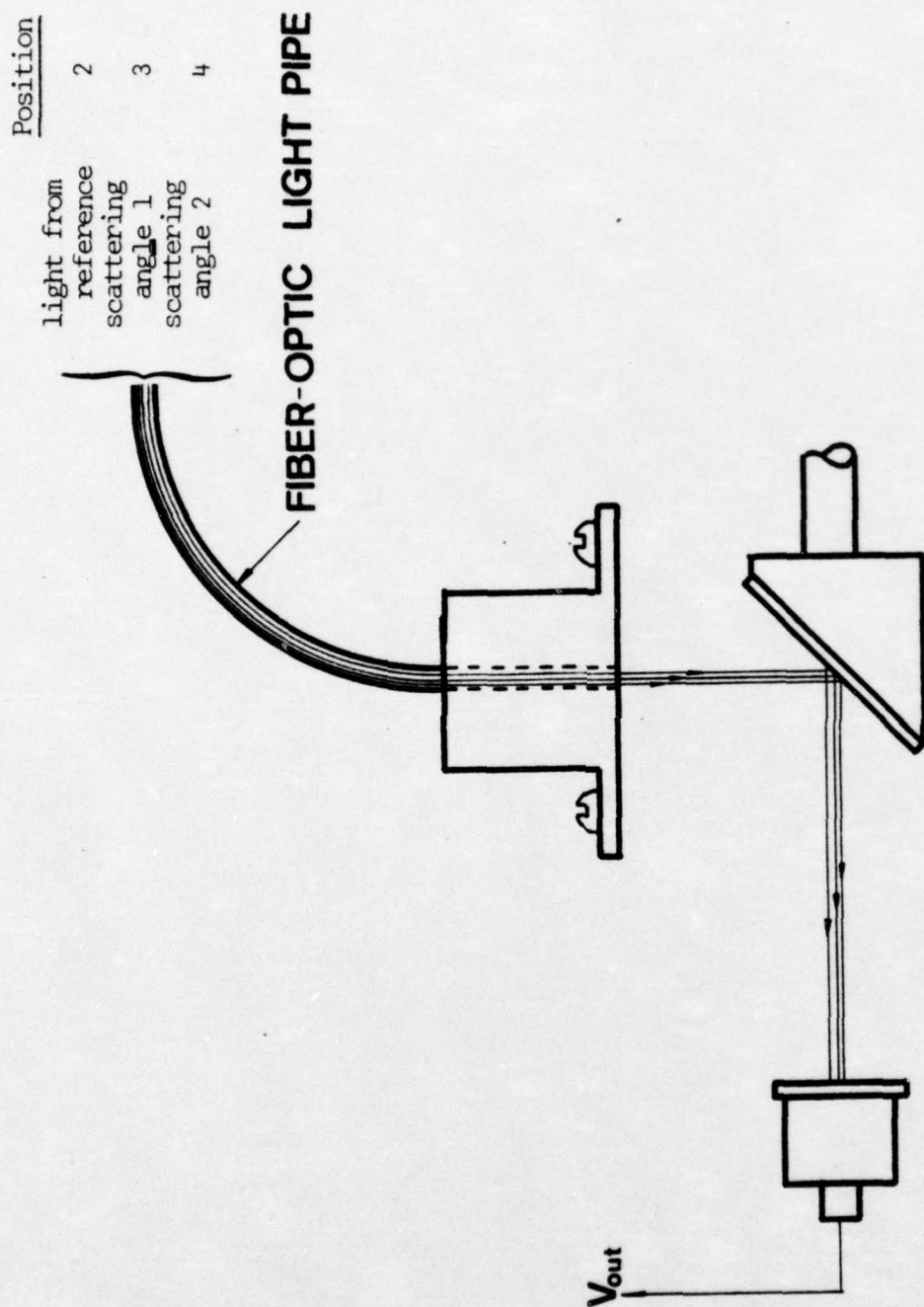


Figure 8. Ray diagram-mirror positions 2, 3 and 4.

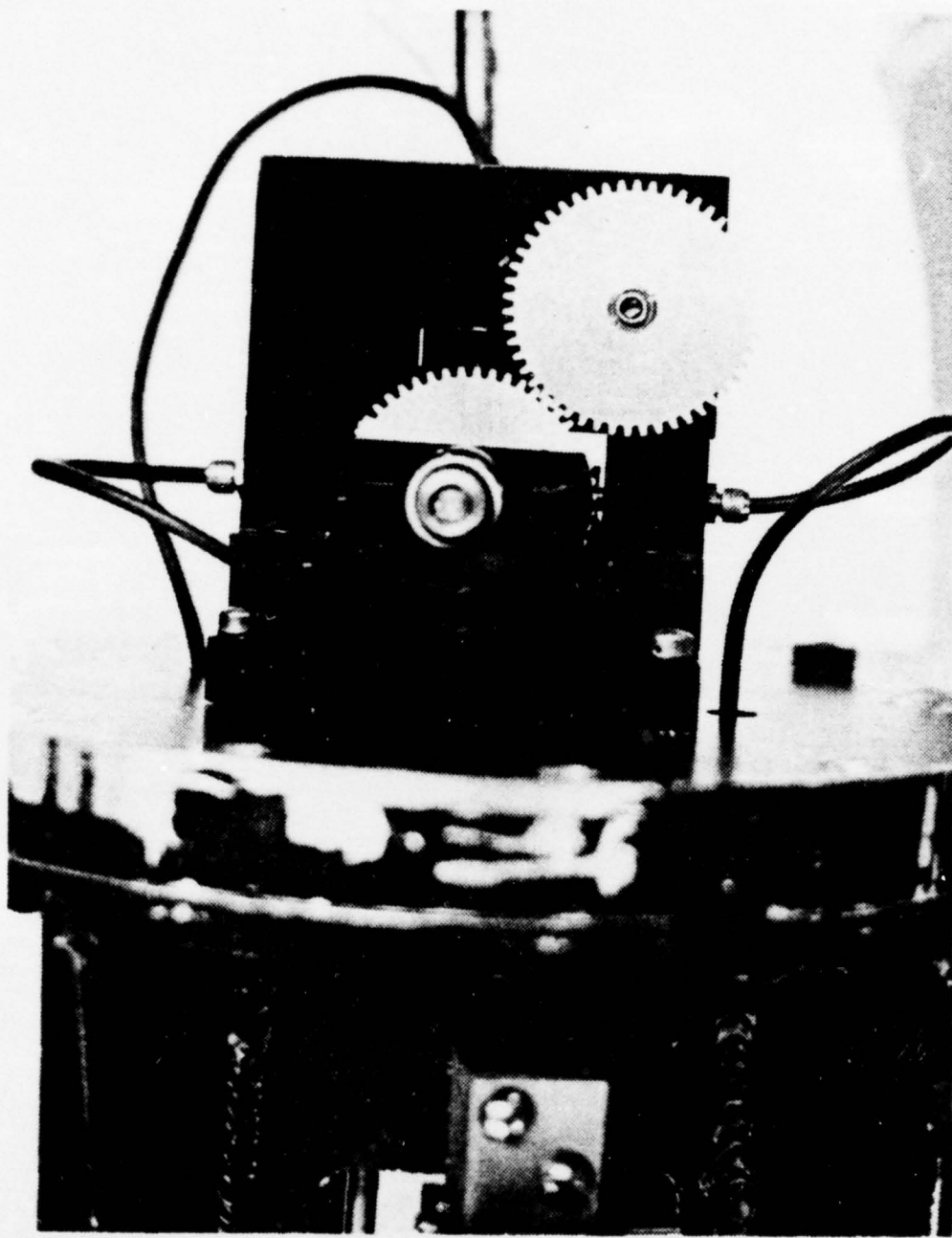


Figure 9. Detector mounting.



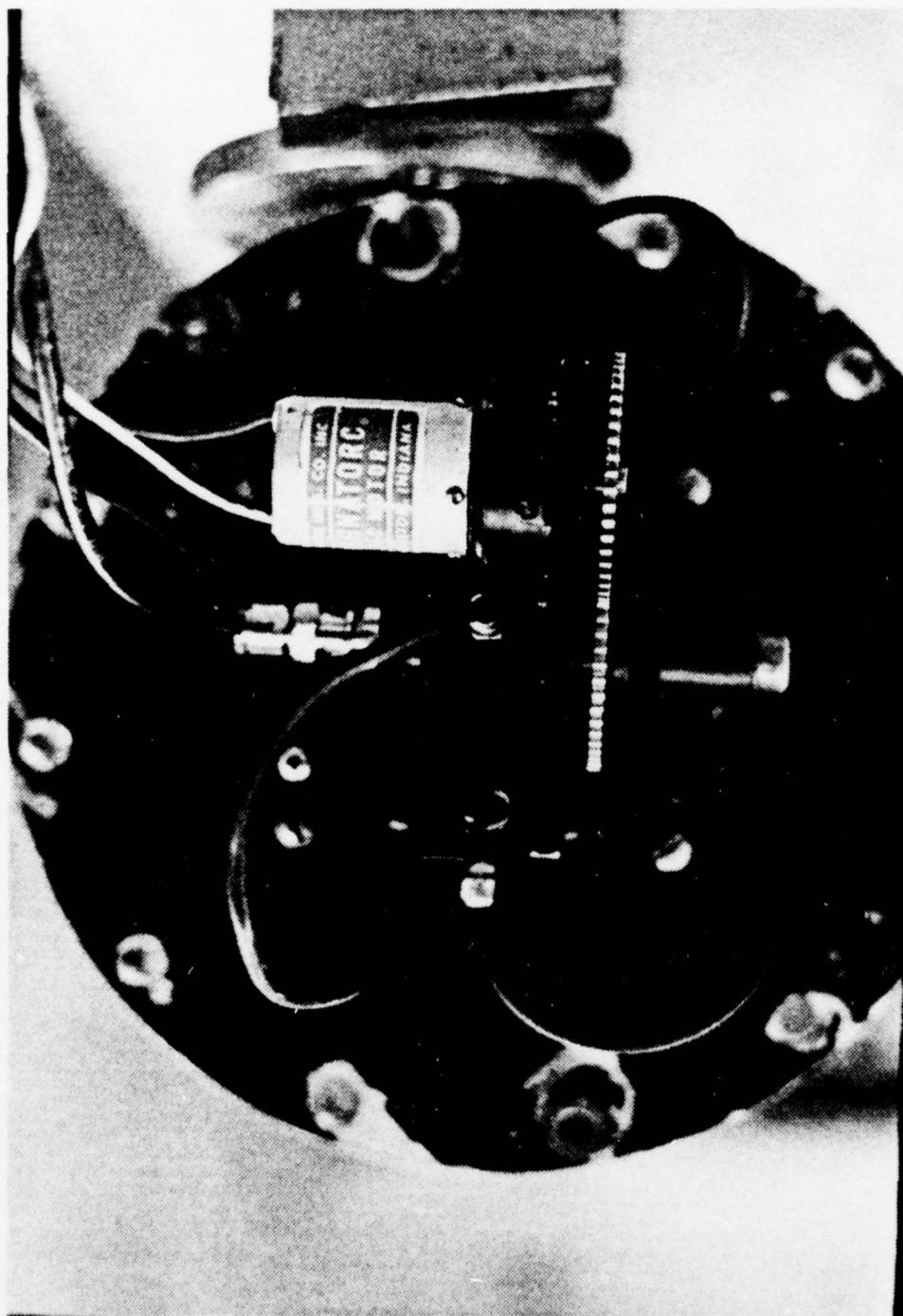


Figure 10. Mirror positioning drive motor.

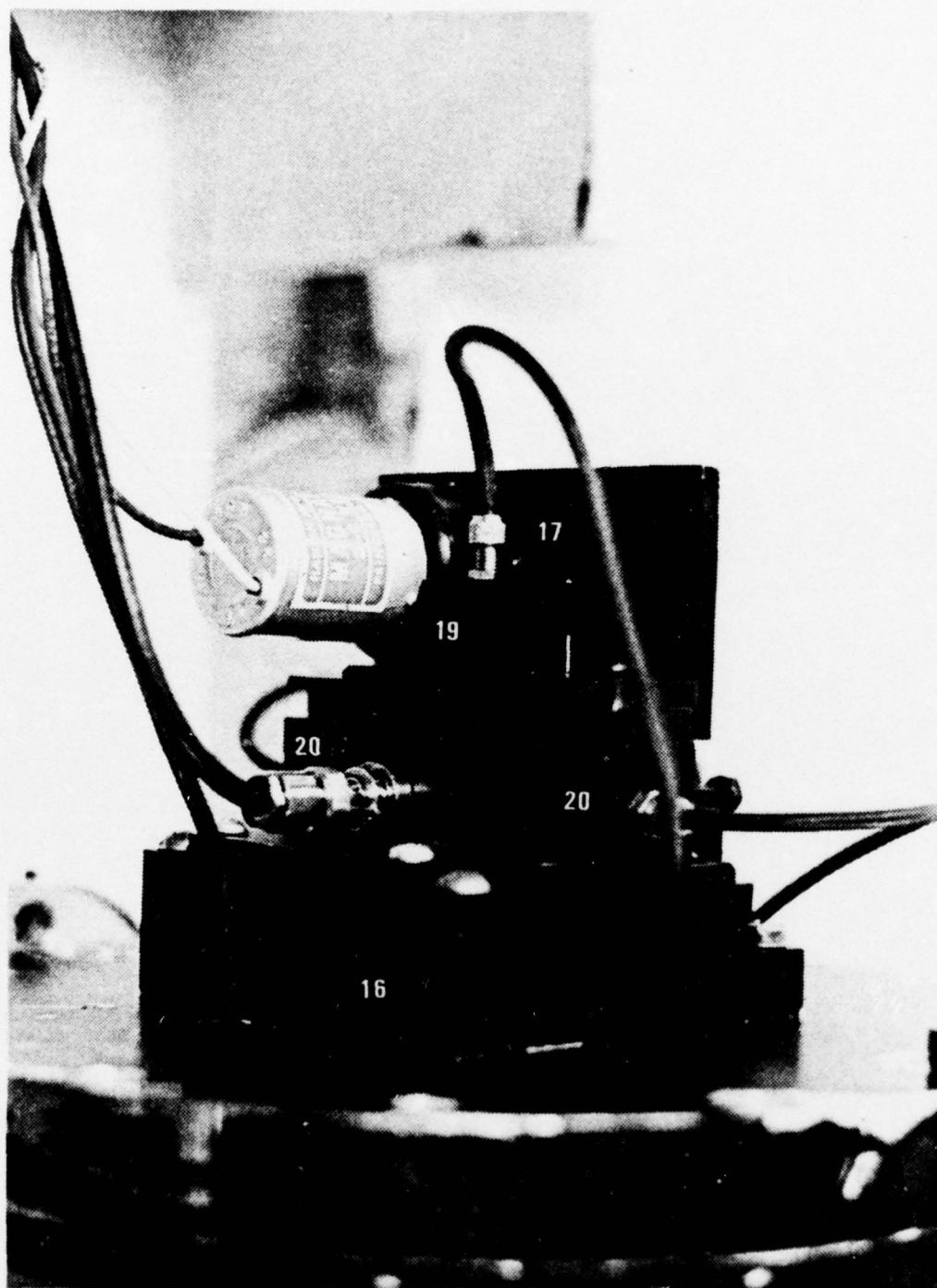


Figure 11. Photodetector mounting arrangement.

### 3. Power Requirements

The instrument requires a low-voltage source capable of providing a maximum of 24 volts and 3 amperes. Figure 12 is a wiring diagram of the underwater electrical connector. Voltages supplied to pins 3, 4, 5 and 6 of this connector via a supply cable power the lamp and D.C. motor. The motor requires 24 volts to drive it at 42 rpm. In tests conducted in the laboratory, a supply of 6 volts was sufficient to provide 10 samples per minute. Rotation rates greater than 42 rpm may be obtained by changing the drive gears. Pins 3 and 6 are for the motor supply.

The power for the G.E. 1974 lamp is supplied through pins 4 and 5. No polarity need be observed on the lamp supply.

There is sufficient room provided in the pressure case that surrounds the detector to install a fixed battery supply should this become necessary. However, the cable to the ship makes it possible to change supply voltages and thus the lamp intensity and motor speed.

### 4. System Operation

Figure 13 is a conceptual diagram depicting the basic operation of the instrument. The rotating diagonal mirror sequentially reflects the light coming from four different sources, into the solid state detector. Three of these sources represent quantities to be measured and the fourth is the lamp reference input. Figures 14 and 15 show the scattering sensor arrangement in side and top views, respectively.



Hansen Magnatorc motor  
(42 rpm at 24v)

lamp  
G.E. 1974 (3a, 6v)

Detector  
UDT PIN-10

MECCA #2047

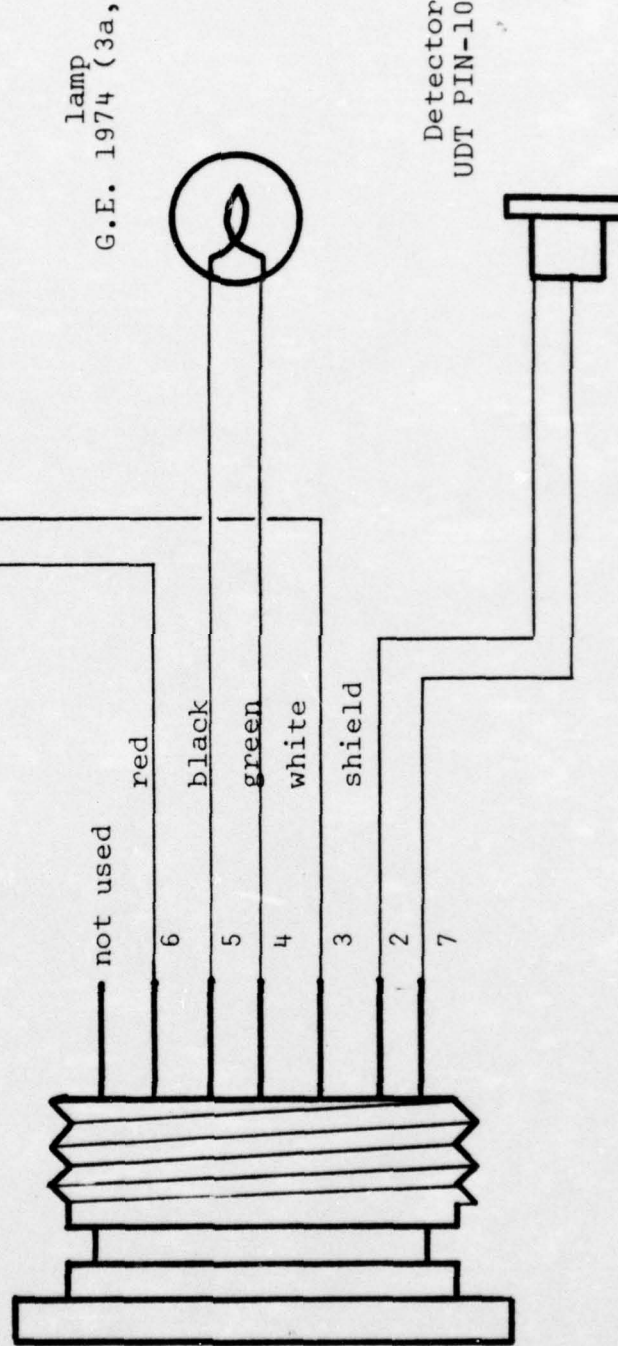


Figure 12. Underwater electrical connector wiring diagram.

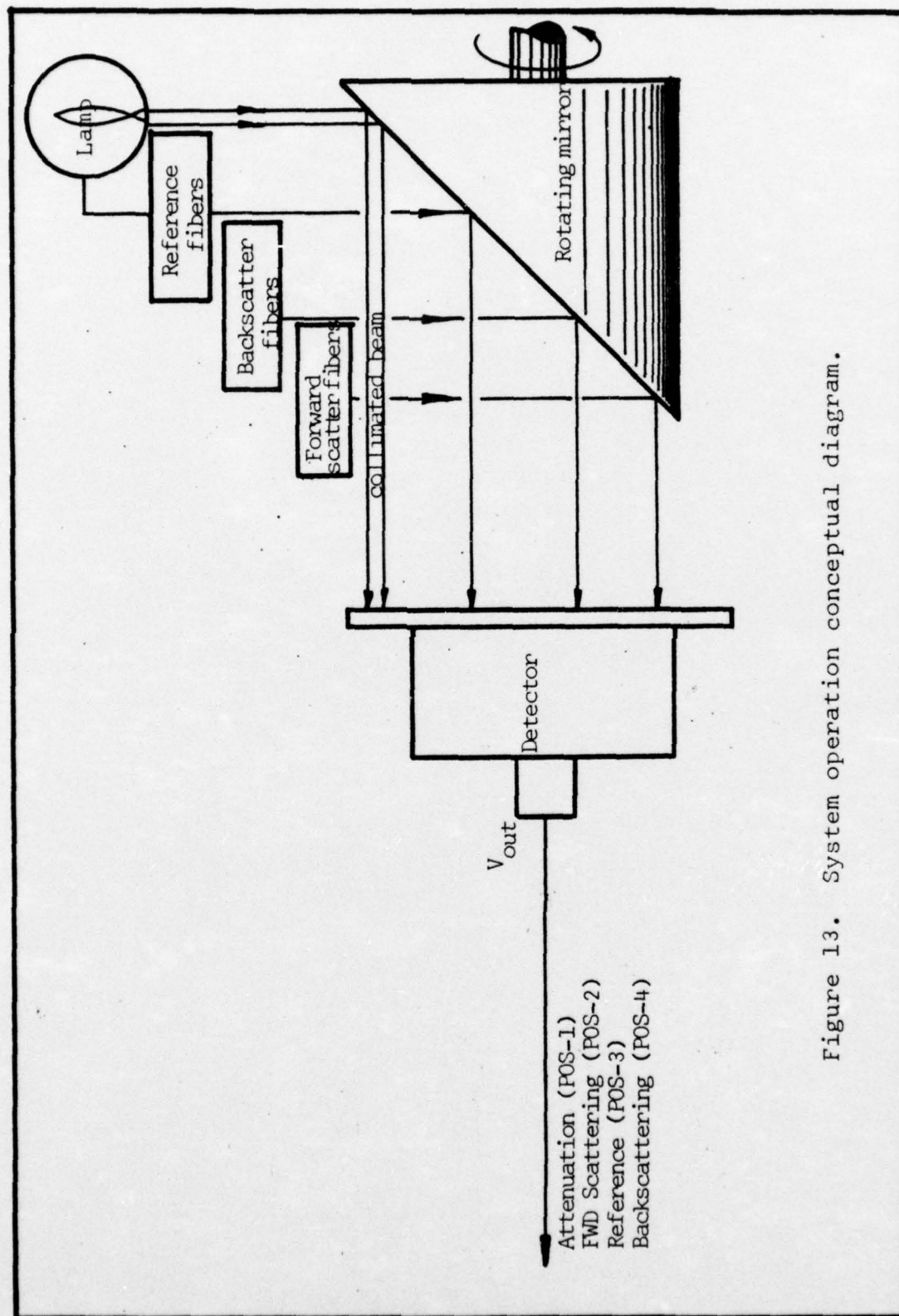


Figure 13. System operation conceptual diagram.

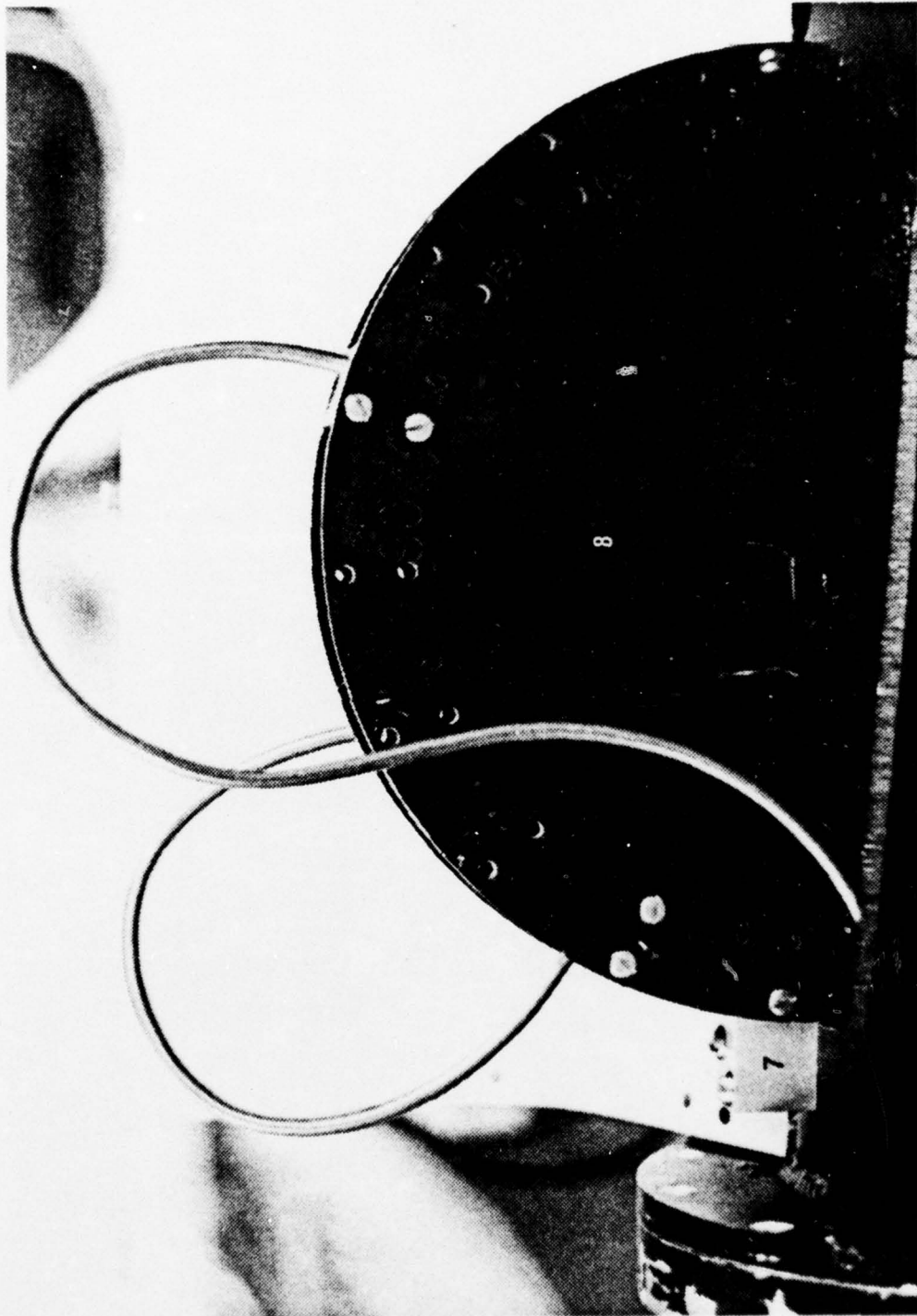


Figure 14. Scattering sensor arrangement, side view.



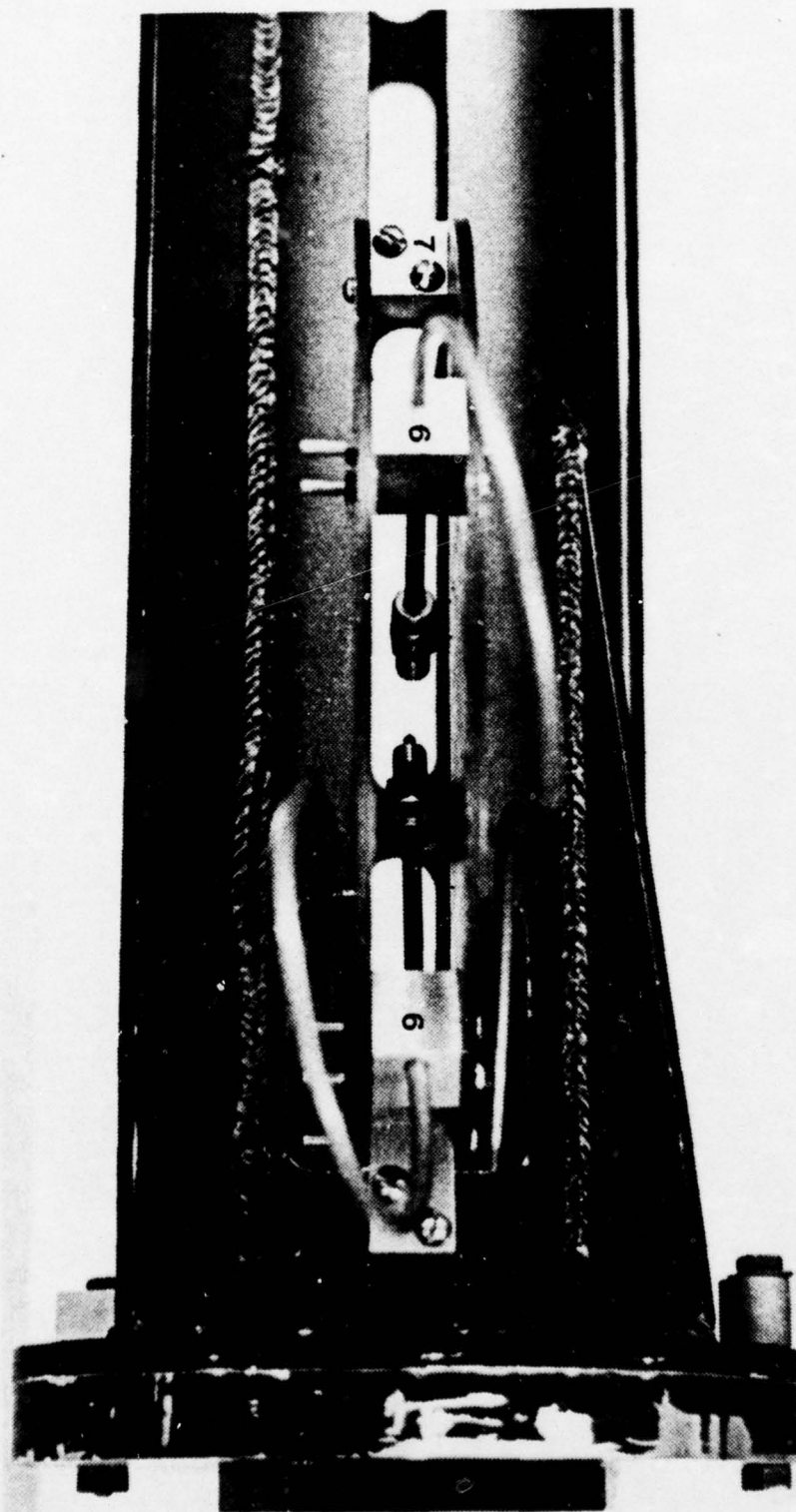


Figure 15. Scattering sensor arrangement, top view.

The detector is operated in a biased mode and gives an output voltage proportional to the input light intensity. Although this method of operation increases detection sensitivity, a dark current exists which must be dealt with during data analysis. A Wratten 61 filter was installed in front of the detector for the purpose of restricting the wavelengths of light admitted to a bandwidth of about 60 nm having a dominant wavelength of about 534 nm.

During air calibration the infrared wavelengths must be attenuated, as they are present in the spectrum admitted to the detector, which is sensitive to I.R. Removal of the I.R. wavelengths is best accomplished by using a Schott BG-18 I.R. blocking filter which was unavailable during the initial laboratory set-up. Instead, a Corning 1-57 filter was used in conjunction with a Hoya HA-30. The total system is shown in Figure 16 with the pressure housings removed for clarity.

#### 5. Output

The detector output (Figure 17) is an analog voltage signal representing each property measured: transmission, scattering at angle  $\theta_1$ , reference intensity and scattering at angle  $\theta_2$ . The absence of scattering signals is explained by noting that the meter was bench operated and the scattering levels are imperceptible in air.

### B. RESULTS

#### 1. Bench Testing

A Gould Model 110 recorder was used to obtain a laboratory calibration of the instrument. On the 5-mV scale the maximum signal level was 2.25 mV.

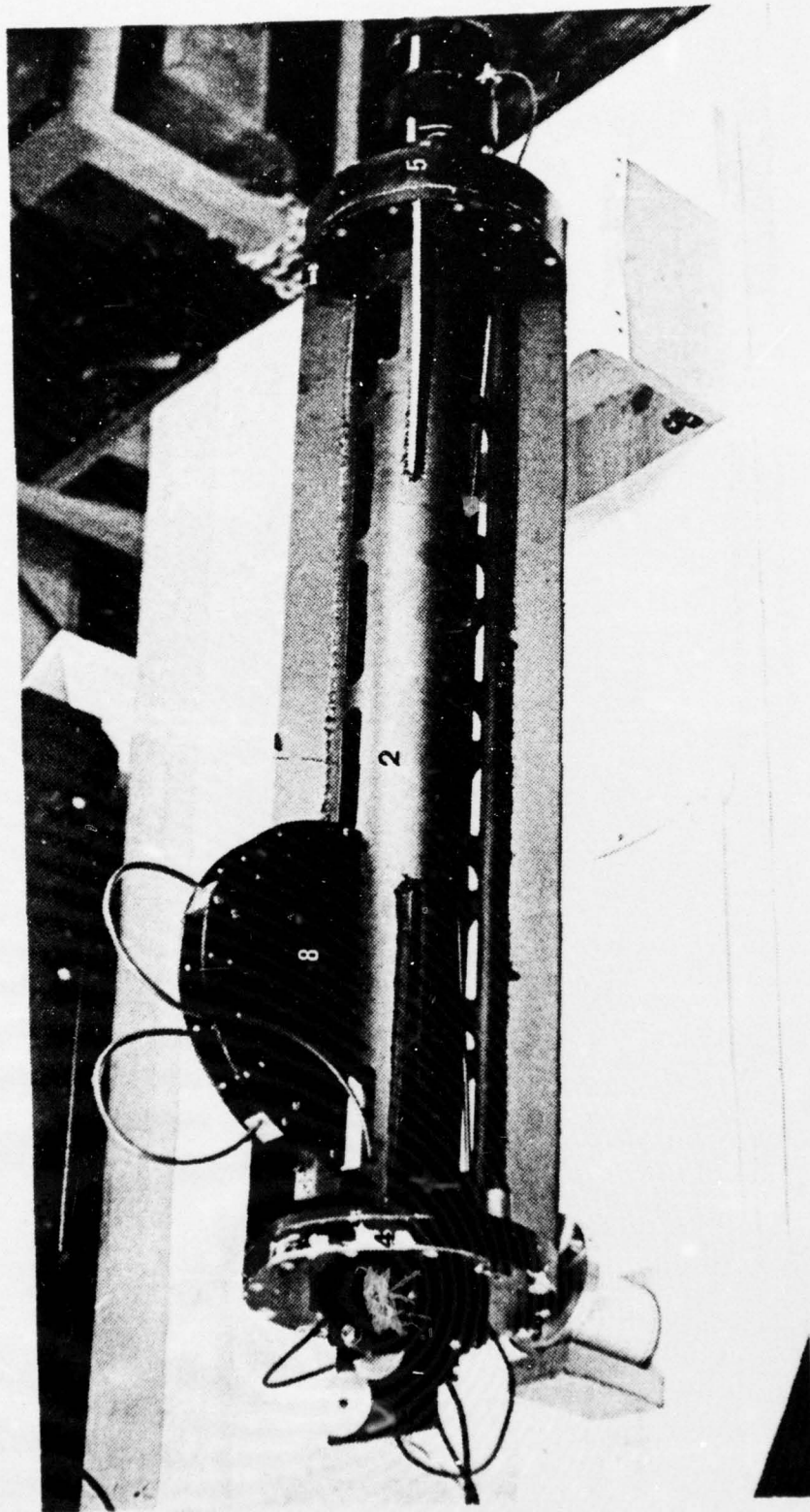


Figure 16. Transmissometer-nephelometer system.



A motor reversing switch was used to stop the mirror in a position where maximum transmission occurred. The recorder signal of 2.25 mV corresponds to 92.5% transmission in water. Wratten neutral density filters were used to verify the detector linearity to a known reduction in beam intensity. The calibration was accomplished with the set-up depicted in Figure 18.

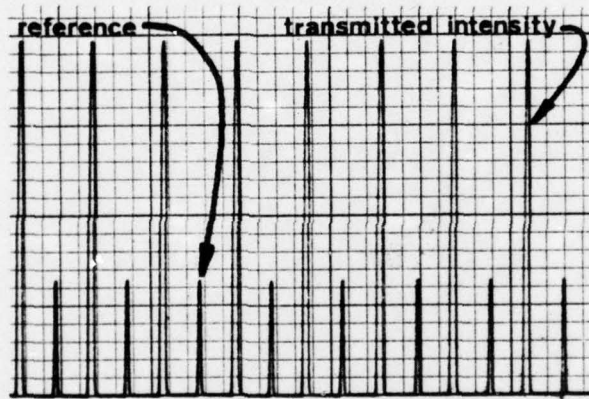


Figure 17. Voltage output; bench operation.

a. Equipment

The following equipment was used for bench tests:

- 1) P/S 1 Hewlett Packard 6215A power supply
- 2) P/S 2 Power Designs 36505 power supply
- 3) P/S 3 Powermate BP34C power supply
- 4) Gould Model 110 Recorder

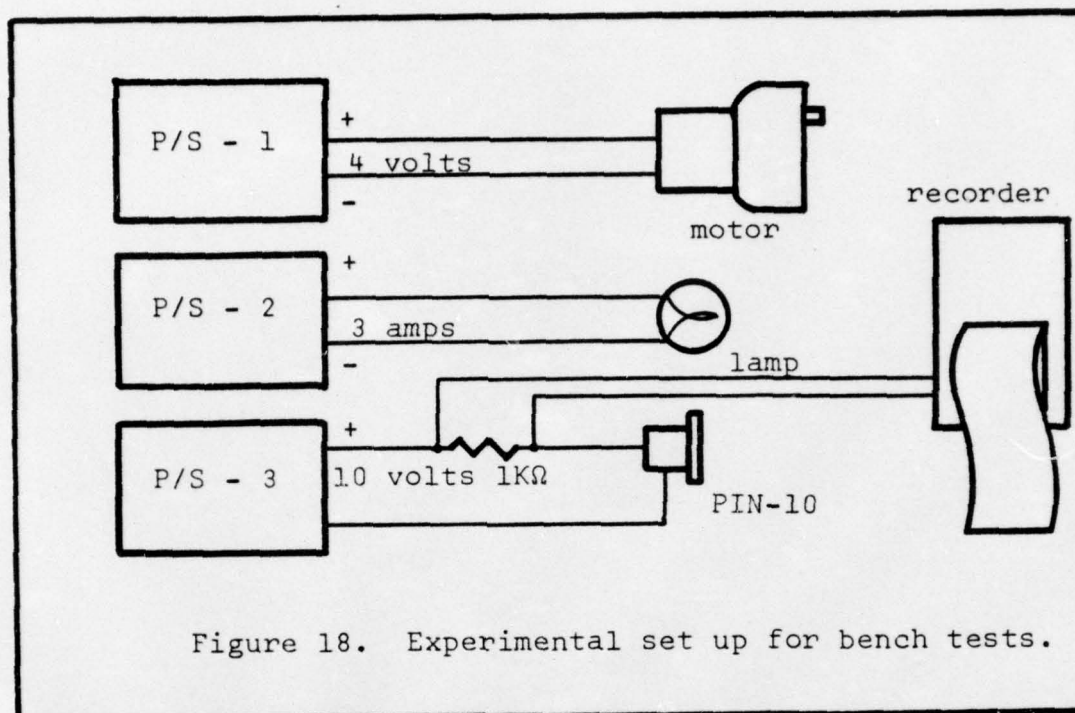


Figure 18. Experimental set up for bench tests.

#### b. Optical Filters

- 1) Wratten 61; installed in detector face.
- 2) Hoya HA-30 I.R. absorbing filter in lens retainer (P/N 18).

- 3) Corning 1-57 at detector face.

The transmission curves for the Corning 1-57 and Wratten 61 filters are shown in Figure 19. The transmission curve for the Hoya HA-30 filter is shown in Figure 20. The Wratten 61 filter limits the wavelengths to a bandwidth of 60 nm at a dominant wavelength of 534 nm.

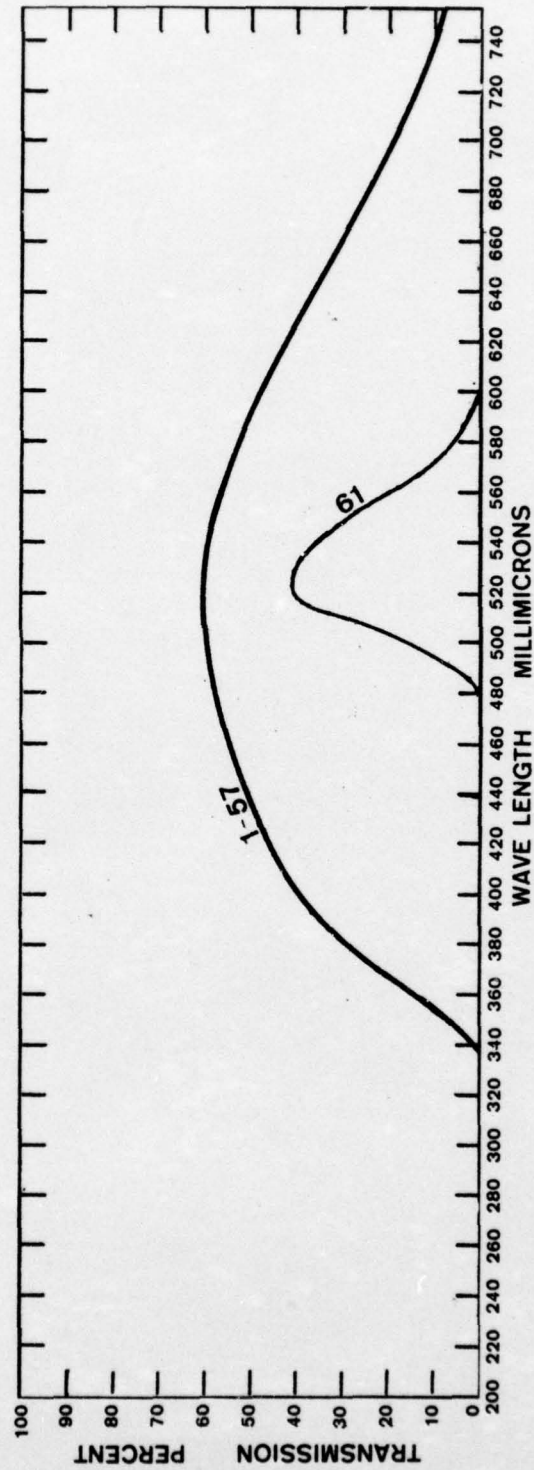


Figure 19. Transmission curves for Corning 1-57 and Wratten 61 filters.



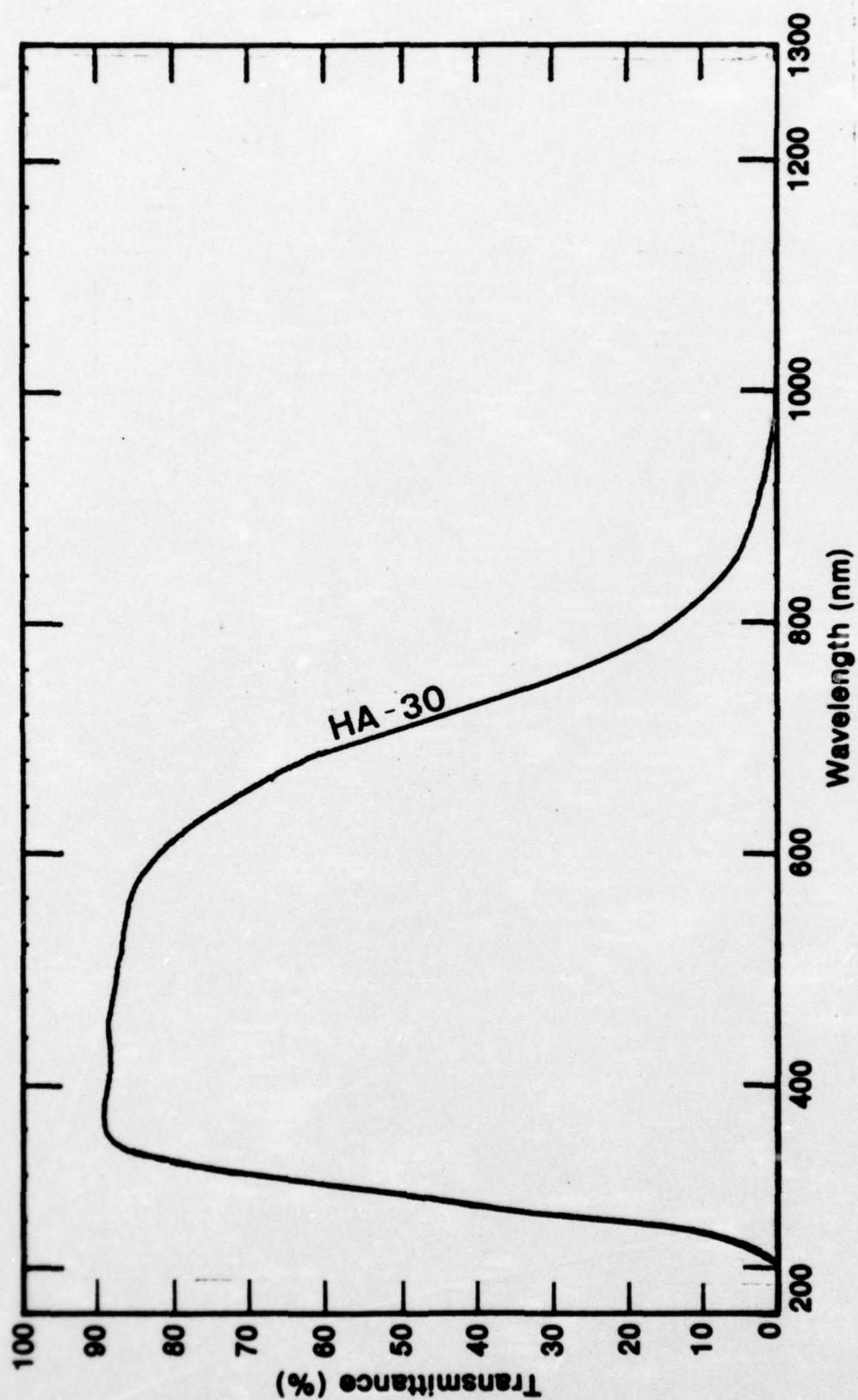


Figure 20. Transmission curve for Hoya HA-30 filter.

c. Detector Biasing

The detector biasing arrangement is shown in Figure 21.

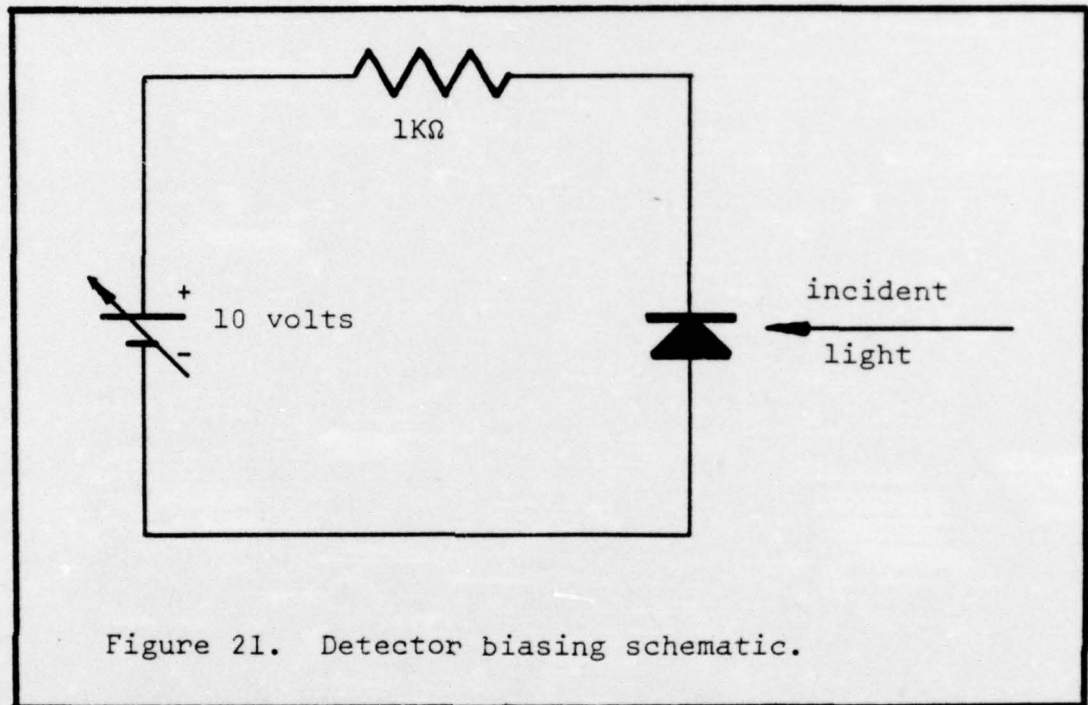


Figure 21. Detector biasing schematic.

During bench testing, a decade resistor substitution box was used in conjunction with the variable power supply to obtain a suitable signal. A bias of 10 volts (as per manufacturers recommendations) was adequate for satisfactory operation.

2. Environmental Testing

On 16 September 1976, the instrument and laboratory apparatus were transported aboard R/V Acania, the Oceanographic research vessel of the Naval Postgraduate School. A 7-meter cast to verify meter operation in an ocean environment was performed. The ship was berthed at the Coast Guard pier in

Monterey Harbor, Monterey, California. This location provided good conditions for the observation of scattered light, as the harbor is a biologically active region having an abundance of dissolved and suspended matter. The results are presented in Figure 22.

Depth	Scale Reading (mV)	Transmittance in water	C m <sup>-1</sup>
on deck	2.250	92.50 (in air)	
1.0	0.200	8.22	2.42
2.5	0.250	10.28	2.20
3	0.250	10.28	2.20
4	0.200	8.22	2.42
5	0.250	10.28	2.20
6	0.155	6.37	2.68
7	0.100	4.11	3.11
bottom	0	0	100

Figure 22. In-water test results.

Scattering of the beam was detectable in the 110° fixed angle sensor, but not measurable, as the recorder sensitivity and response were not great enough to provide a useable signal.



### III. CONCLUSIONS

The NPS Transmissometer-Nephelometer performed as expected in the rather turbid harbor water. The scattering signals were anticipated to be extremely low due to the present poor termination of the fiber bundles and the decrease of light intensity at the detector after the installation of the filters.

Several schemes to improve the performance of the instrument are possible.

A. Detector biasing improvements. A circuit arrangement that is suitable for exhibiting the ultimate capabilities of the detector is given in the manufacturer's application notes. It is operated in the biased mode and includes an A.C. amplifier (i.e. UDT FET 100) to increase the detectable output signal.

B. Fiber-optic terminations. The transmission of scattered light to the detector is extremely dependent upon the manner in which the light pipes are terminated. Potting the ends of the fiber bundles in epoxy and polishing the tips to reduce reflections is one method to reduce attenuation at the input sensor. The sensor ends should also be filled with immersion oil ( $n=1.515$ ) to match the refractive indexes of glass and the optical fibers.

Small negative lenses at the detector end of the sensor input could serve to increase the area of the detector

illuminated. The active area of the PIN-10 detector is  $1.250 \text{ cm}^2$  and should be fully utilized to obtain maximum output signal.

C. Better fibers. The installation of Bausch and Lomb series 32-01, 02 or 03 light "wires" which have been commercially terminated would enhance the light transmission. These non-coherent "wires" have an incident light gathering efficiency of 60% at the receiving end and a transmitting efficiency of 95% per foot.

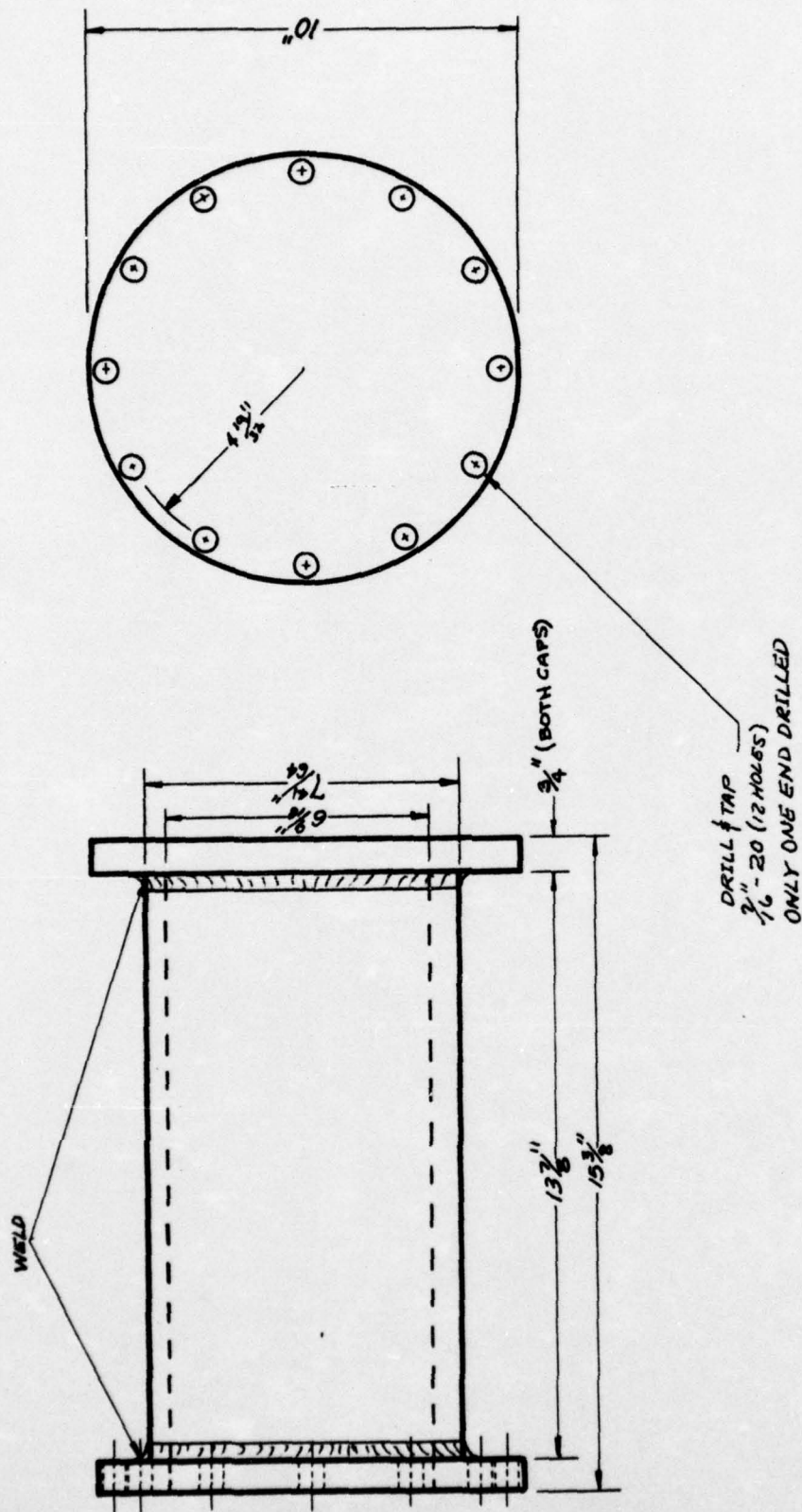
D. Photomultiplier tube. Replacing the PIN-10 detector with a photomultiplier tube and a logarithmic amplifier would provide considerably more output signal. This is especially useful when scattering signals are very low.

E. Chopper relays. The addition of a series of chopper relays synchronized with the rotating mirror may be used to separate electrically the signals representing  $I(0)$ ,  $I(1)$ ,  $\beta(\theta_1)$ , and  $\beta(\theta_2)$ . These signals may then be recorded on separate channels of a tape recorder to simplify analysis.

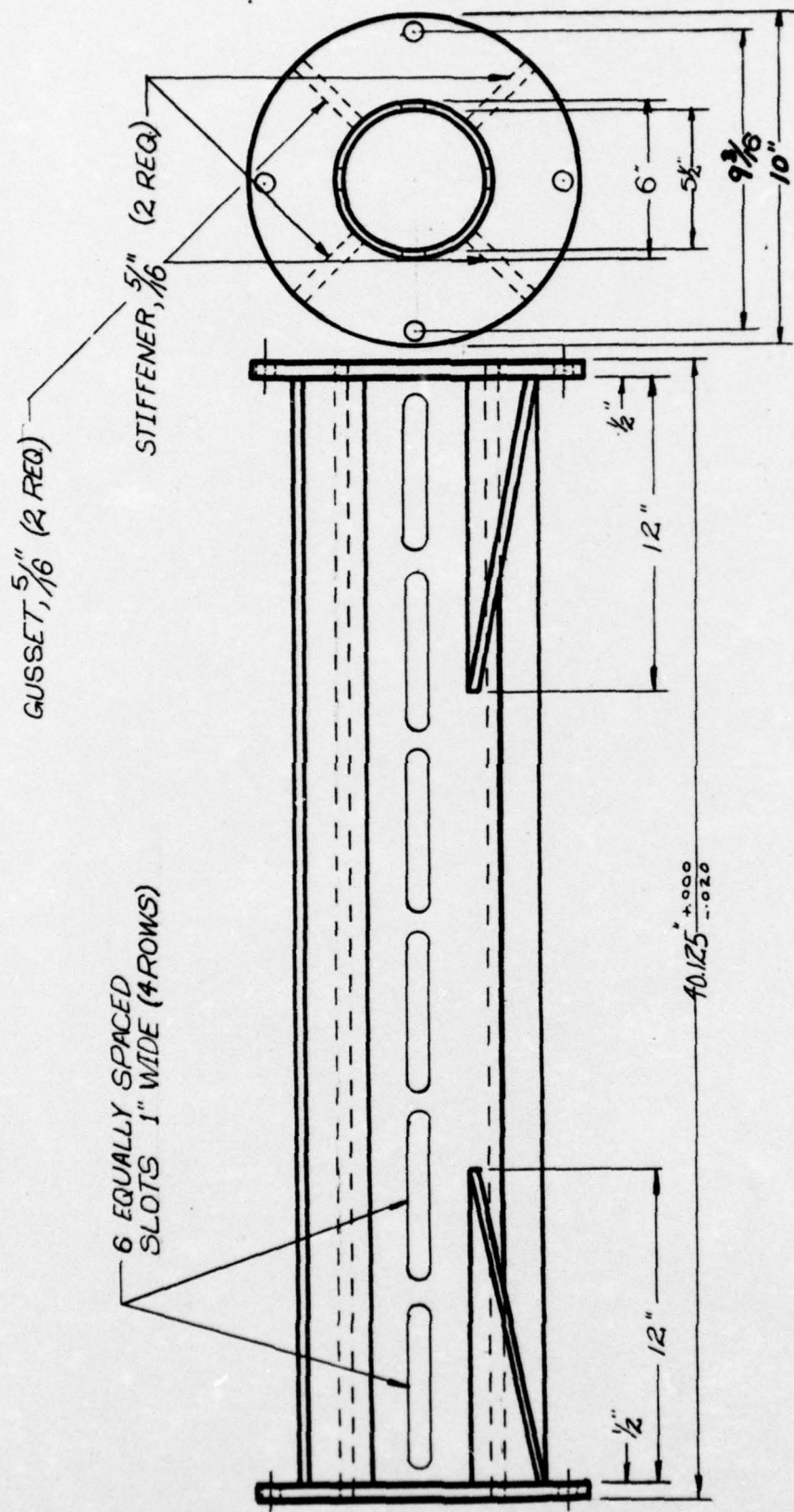
F. Data processing. Improved results can also be obtained through the use of digital processing technique. The analog signals may be recorded on a magnetic tape recorder, digitized with an A to D converter, and computer analyzed.

APPENDIX A  
NPS TRANSMISSOMETER-NEPHELOMETER  
DRAWINGS AND SPECIFICATIONS

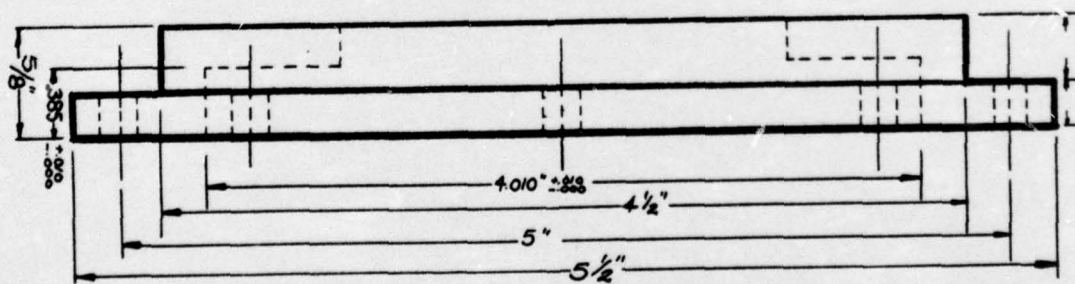
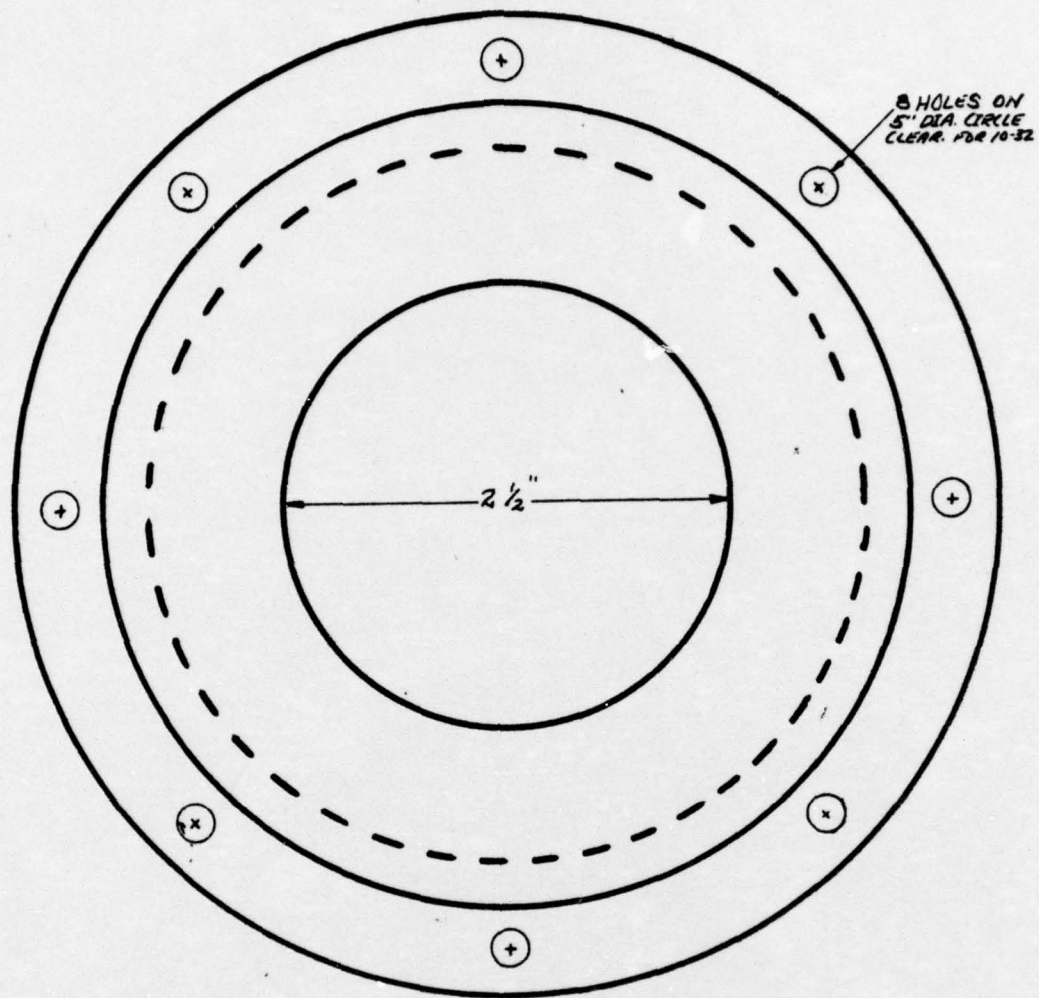




HOUSING, PRESSURE P/L  
MATERIAL: STAINLESS STEEL  
DRAWN BY: LT. D.M. MOSEY  
24 AUGUST 1976 NFE

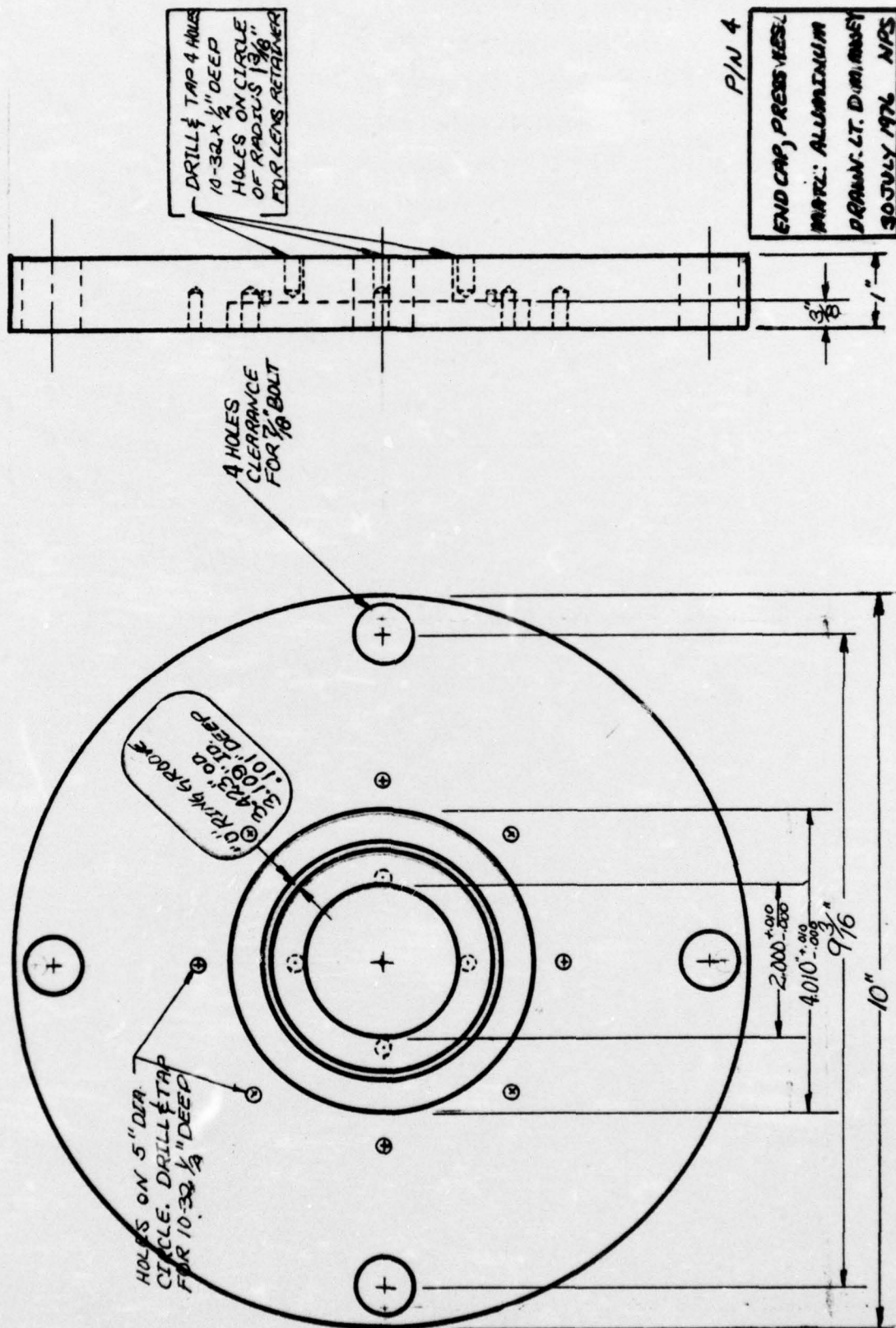


SUPPORT FRAME #N 2  
 MATERIAL: ALUMINUM  
 DRAWN BY: LT. D.M. MOSEY  
 20 JULY 1976 NRS



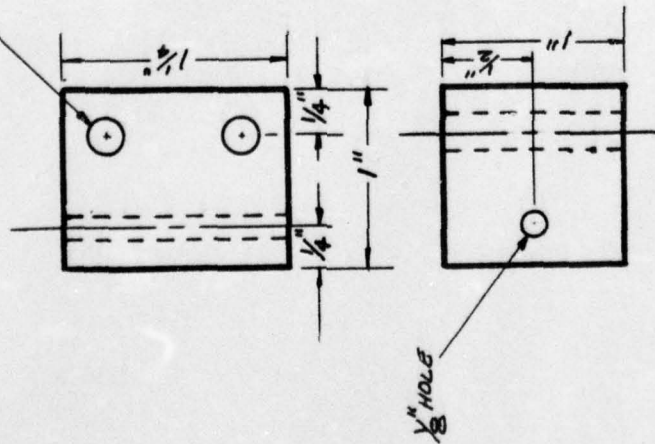
RETAINER, WINDOW P/N 3  
 MATERIAL: ALUMINUM  
 DRAWN BY: LT. D.M. MOSEY  
 30 JULY 1976 NPS





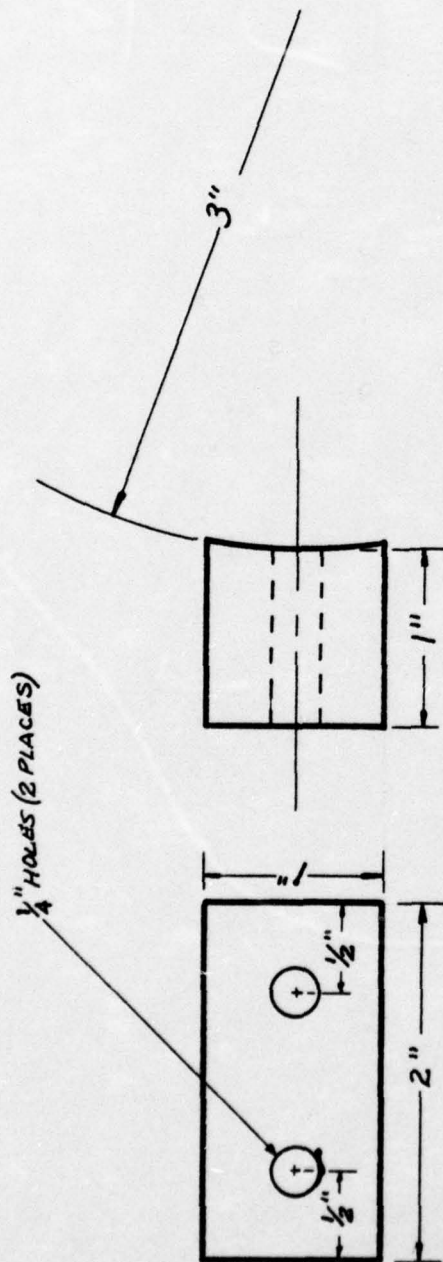


3/16" HOLE (2 PLACES)



MOUNT, FIBRE OPTIC P/N 6  
 MATERIAL: ALUMINUM  
 DRAWN BY: LT D. M. MOSEY  
 24 AUGUST 1976 NPS

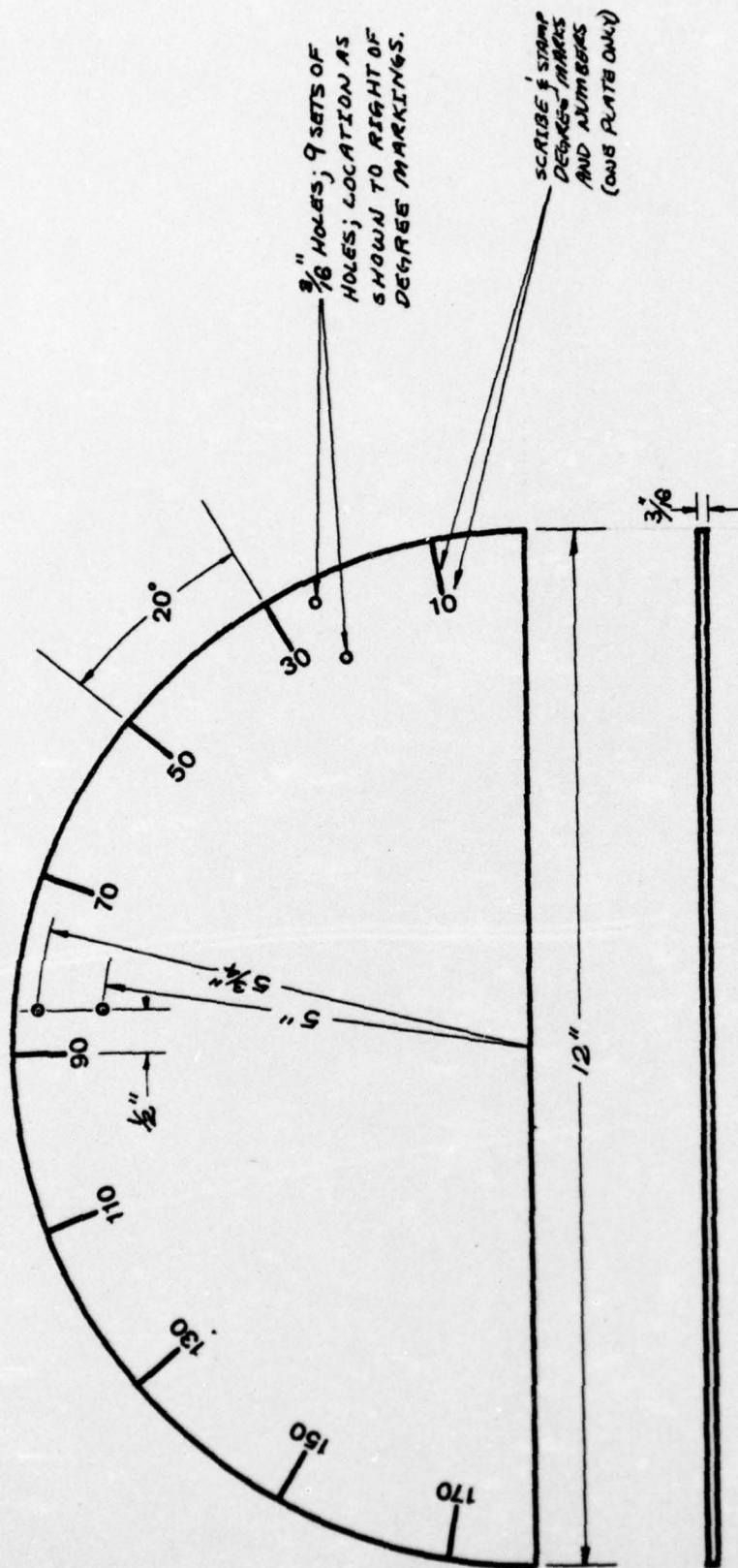




2 REQUIRED

P/N 7

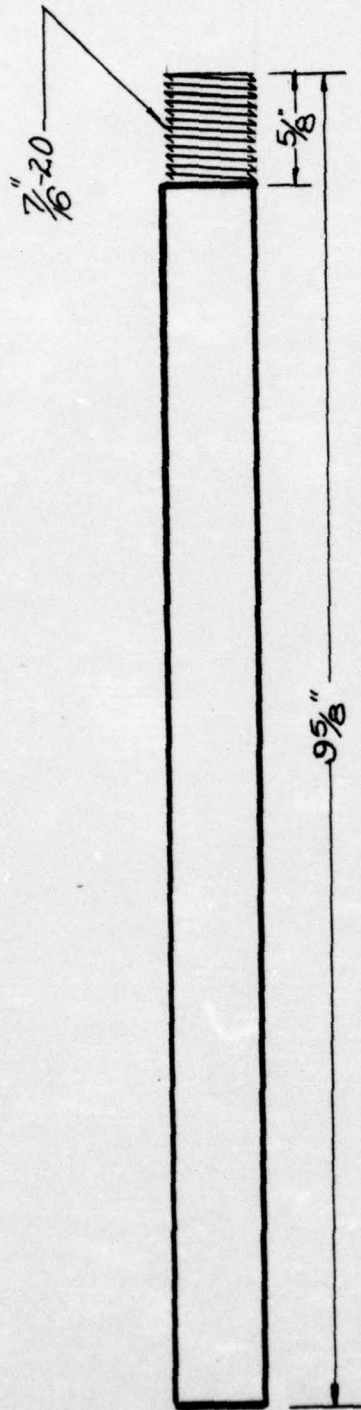
MOUNTING BRACKET, PLATE
MATERIAL: ALUMINUM
DRAWN BY: LT D.M. MOSEY
24 AUGUST 1976 NPS



TWO PLATES REQUIRED

P/N 8

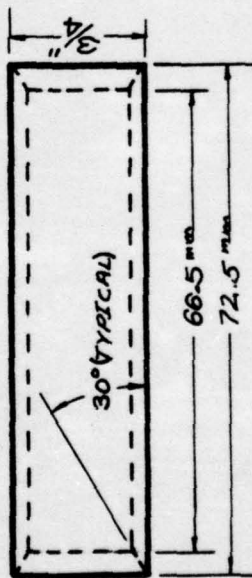
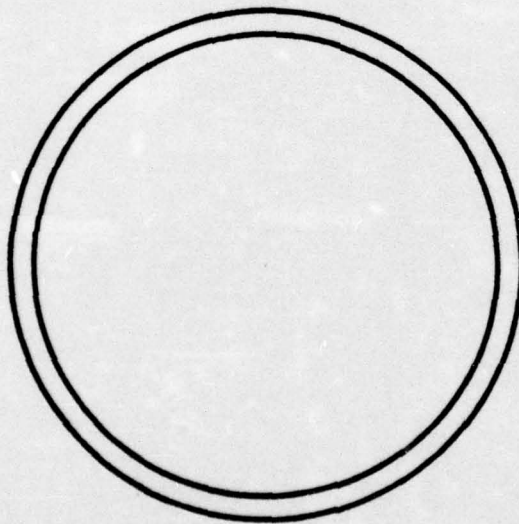
PLATE, MOUNTING, FIXED ANGLE  
MATERIAL: 3/16" ALUM. SHEET  
DRAWN BY: LT. D. M. MOSEY  
24 AUGUST 1976 NPS



3 REQUIRED

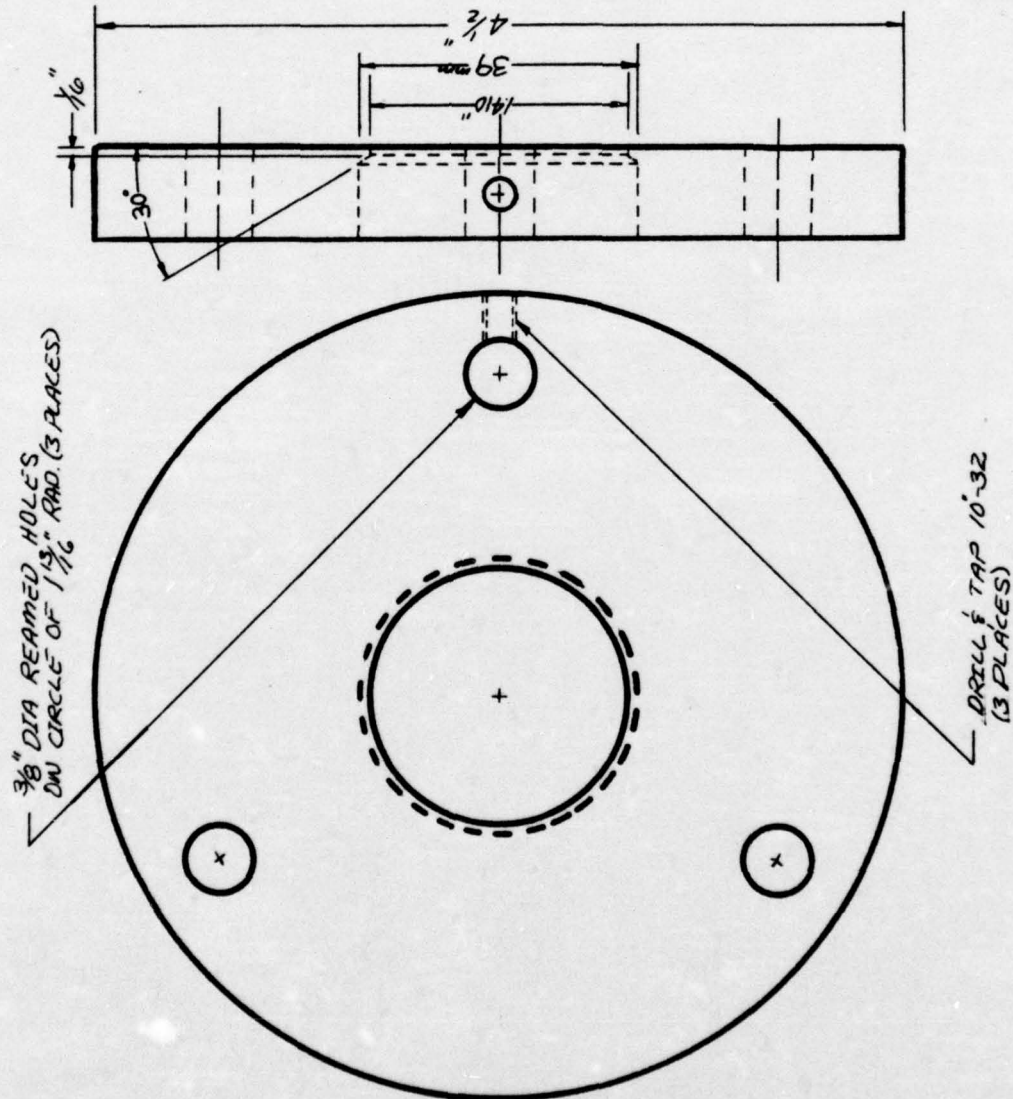
ROD, SLIDER P/N 0  
MATERIAL:  $\frac{1}{2}$ " DIA. STAINLESS  
DRAWN BY: LT D.M. MOSEY  
10 MAY 1976 NPS

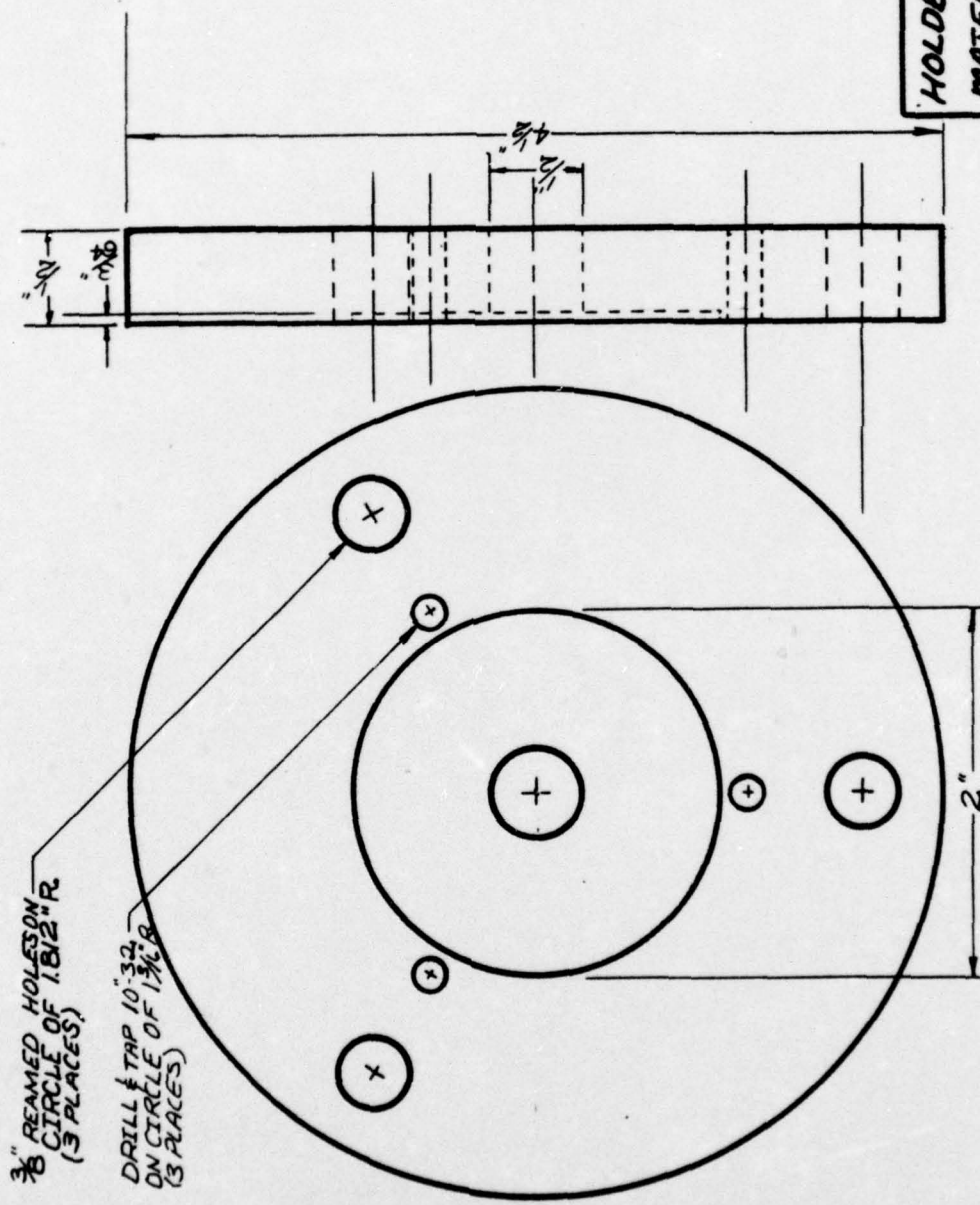




P/N 10  
RING, SPACER, ASPHERIC COND.  
MATERIAL: ALUMINUM  
DRAWN BY: LT. D. M. MOSEY  
12 APRIL 1976 NPS

P/N 11  
 HOLDER, LENS, 39mm  
 MATERIAL: ALUMINUM  
 DRAWN BY: LT. D. M. MOSEY  
 8 APRIL 1976 NPS



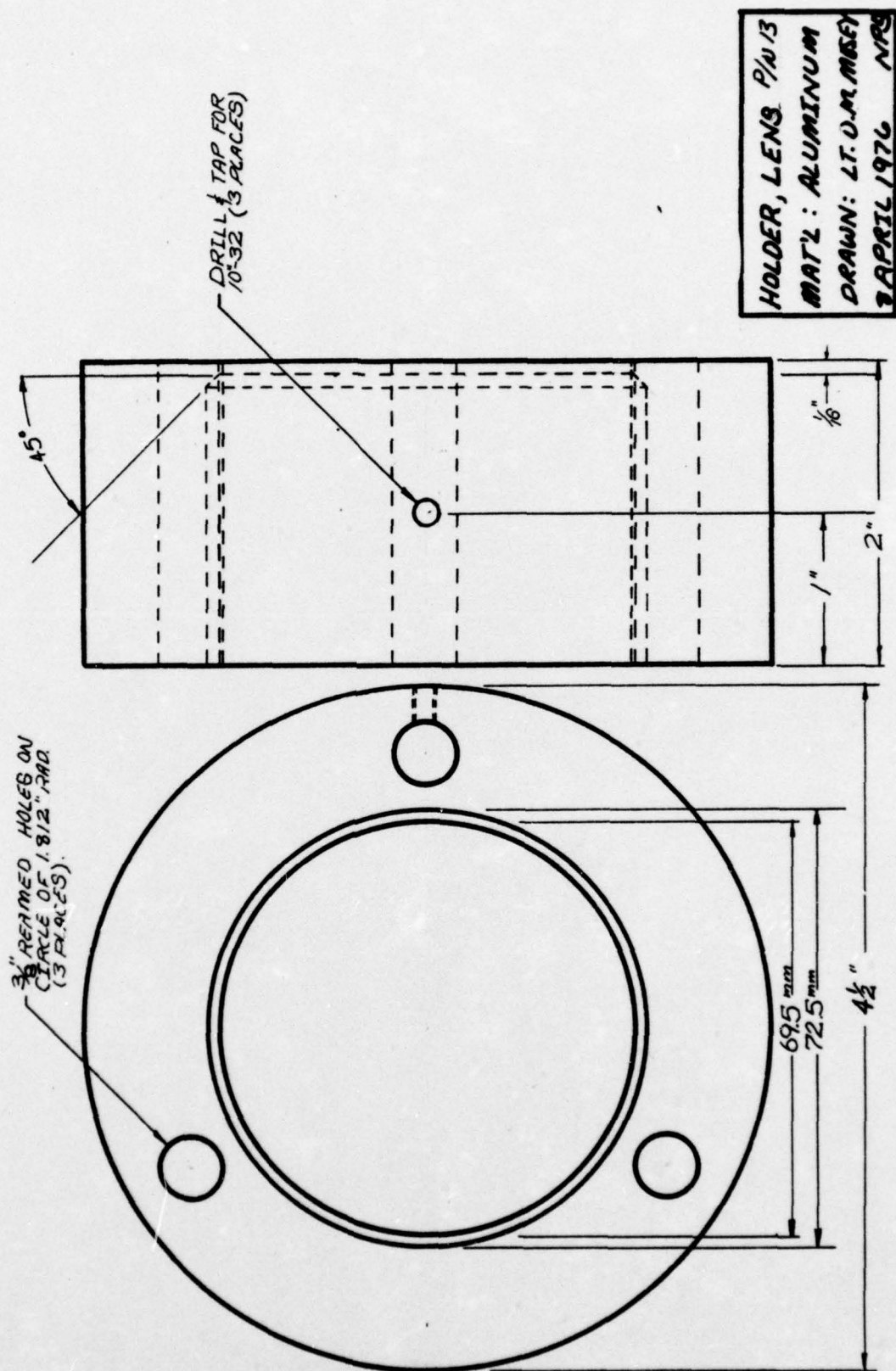


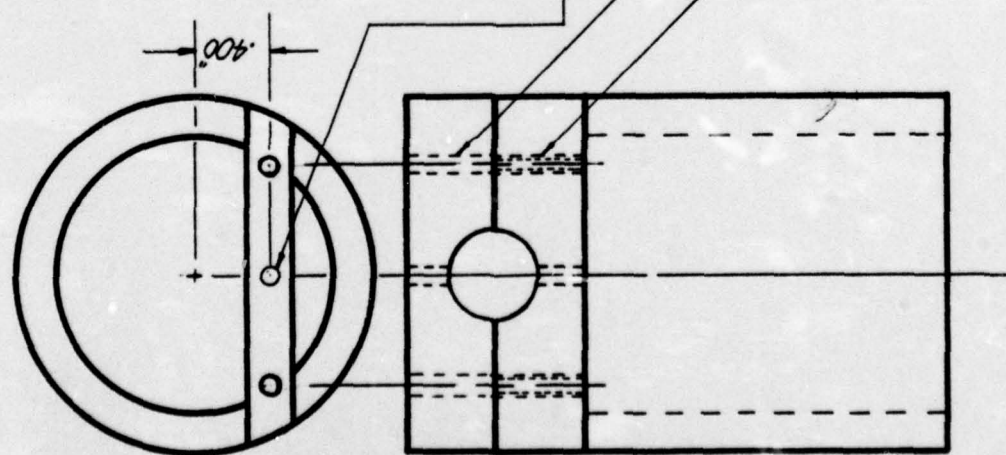
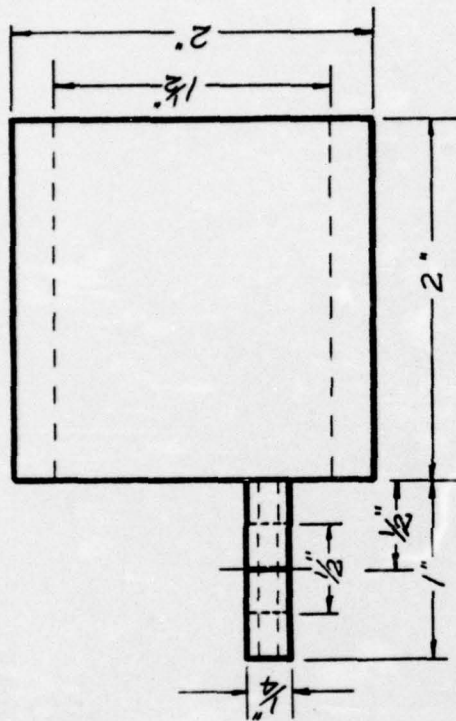
3/8" REAMED HOLES ON  
CIRCLE OF 1 1/2" R  
(3 PLACES)

DRILL & TAP 10/32  
ON CIRCLE OF 1 1/2" R  
(3 PLACES)

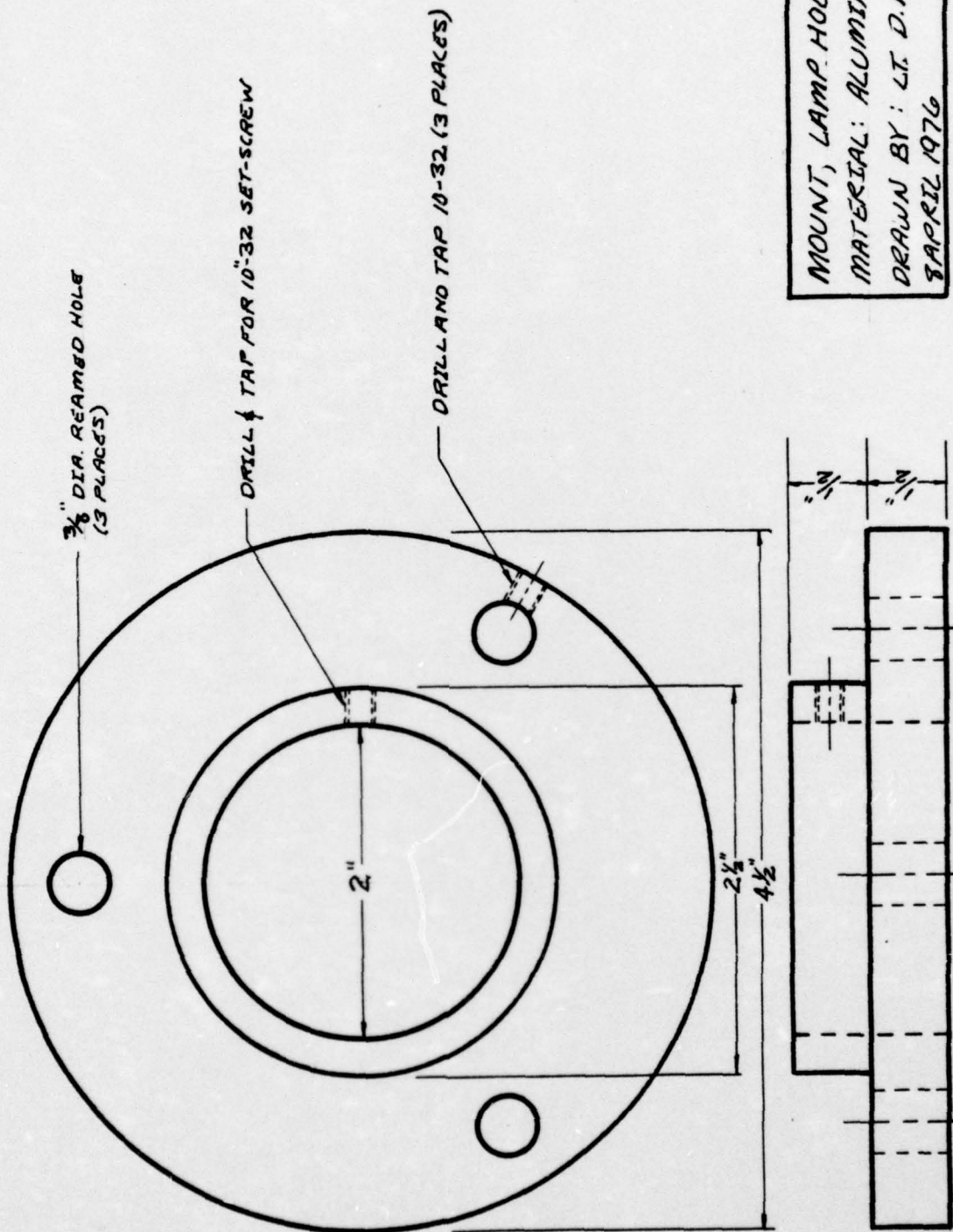
HOLDER, LIGHT STOP P/N 12  
MATERIAL: ALUMINUM  
DRAWN BY: LT. D.M. MOSEY  
13 APRIL 1976  
NPS





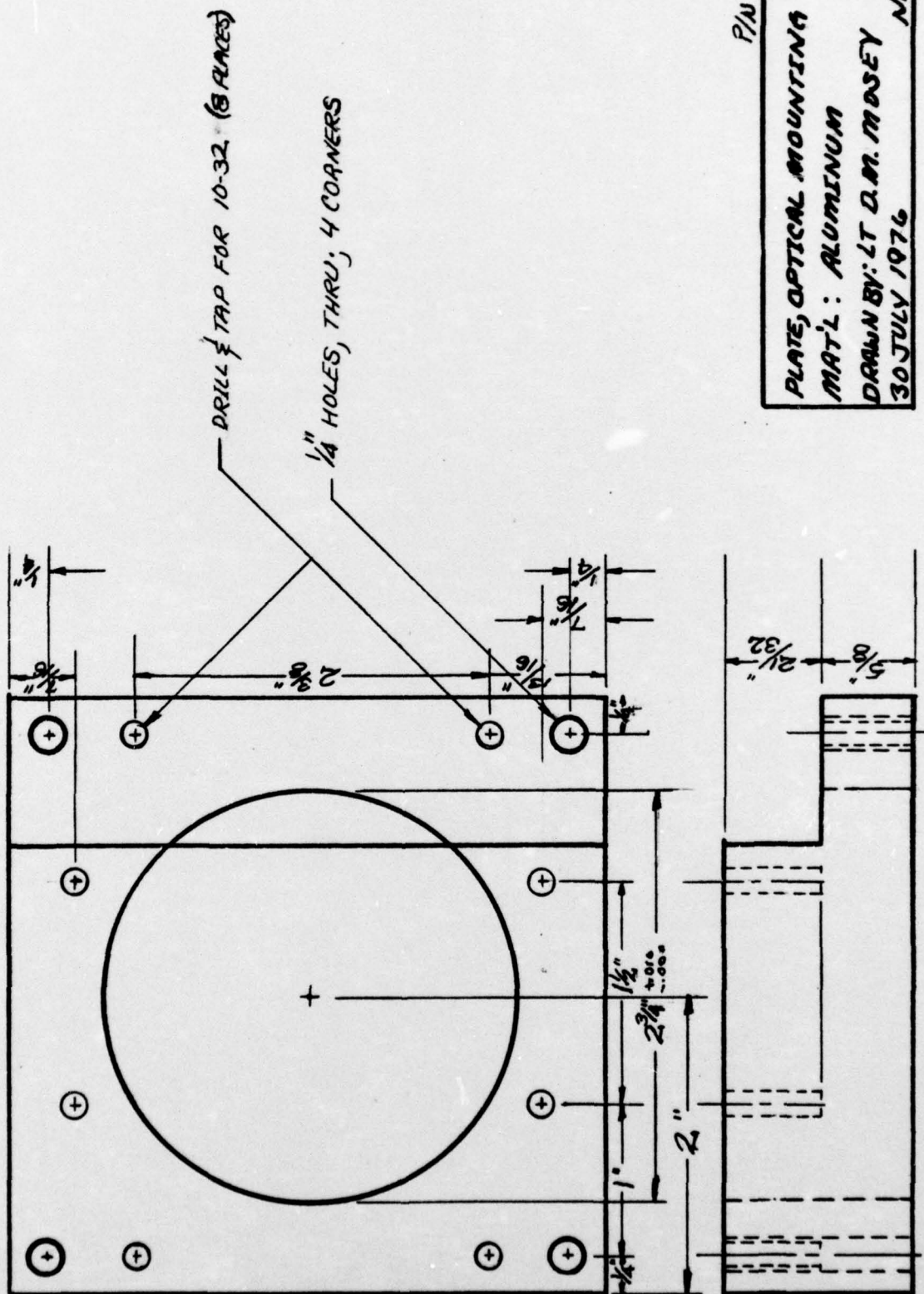


HOLDER, LAMP P/N 14  
 MATERIAL: ALUMINUM  
 DRAWN BY: LT. D.M. MOSEY  
 1 APRIL 1976 NPS



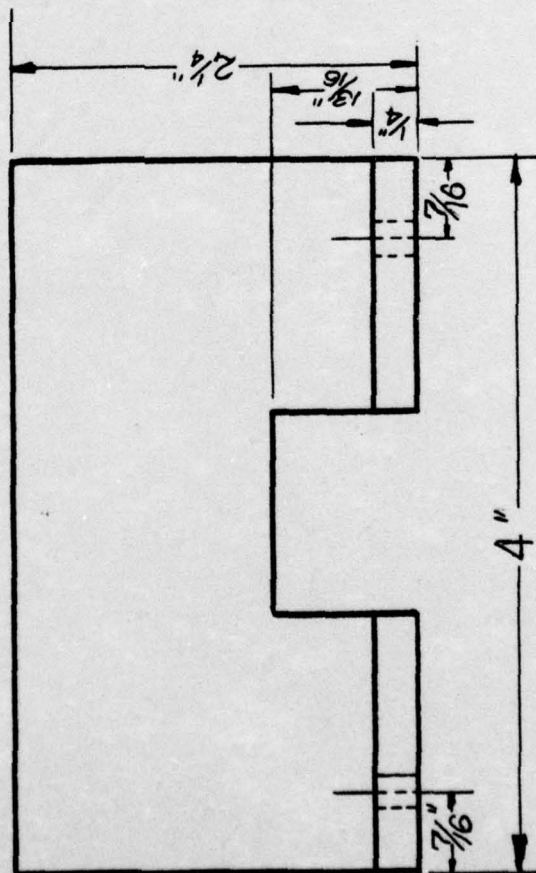
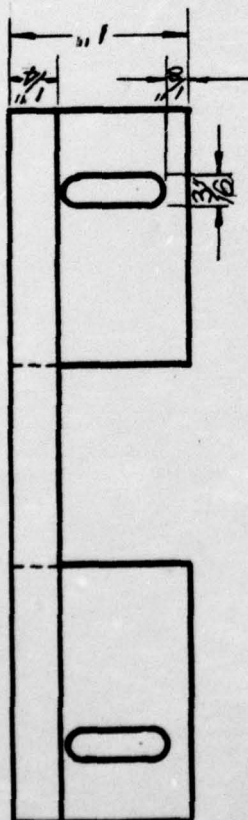
MOUNT, LAMP HOLDER P/W/S  
 MATERIAL: ALUMINUM  
 DRAWN BY: LT. D.M. MOSEY  
 8 APRIL 1976 NPS



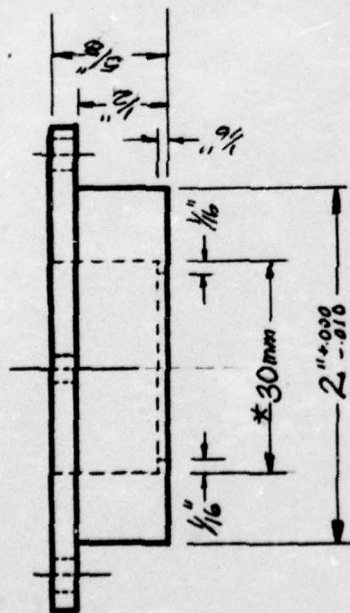


P/N 16

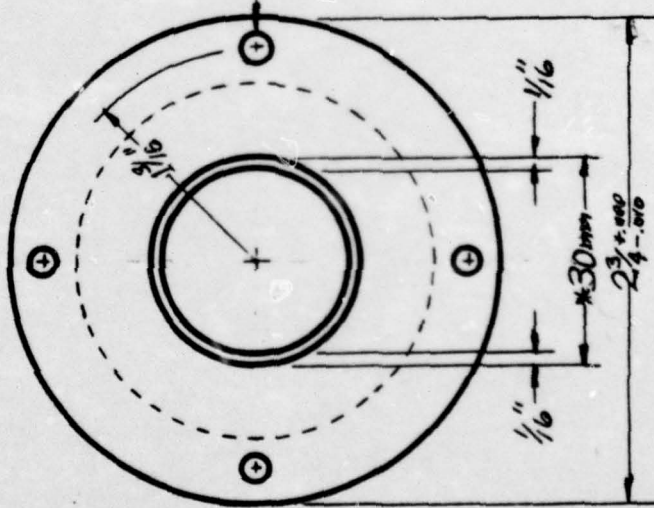
PLATE, OPTICAL MOUNTING  
 MAT'L: ALUMINUM  
 DRAWN BY: LT D.M. MOSEY  
 30 JULY 1976  
 NPS



BRACKET, MOTOR P/N 17  
 MATERIAL: ALUMINUM  
 DRAWN BY: LT D.M. MOSEY  
 30 JULY 1976 NDS



3/16" DIA. HOLES (4 PLACES)  
HOLES ON 1 3/16" DIA. CIRCLE



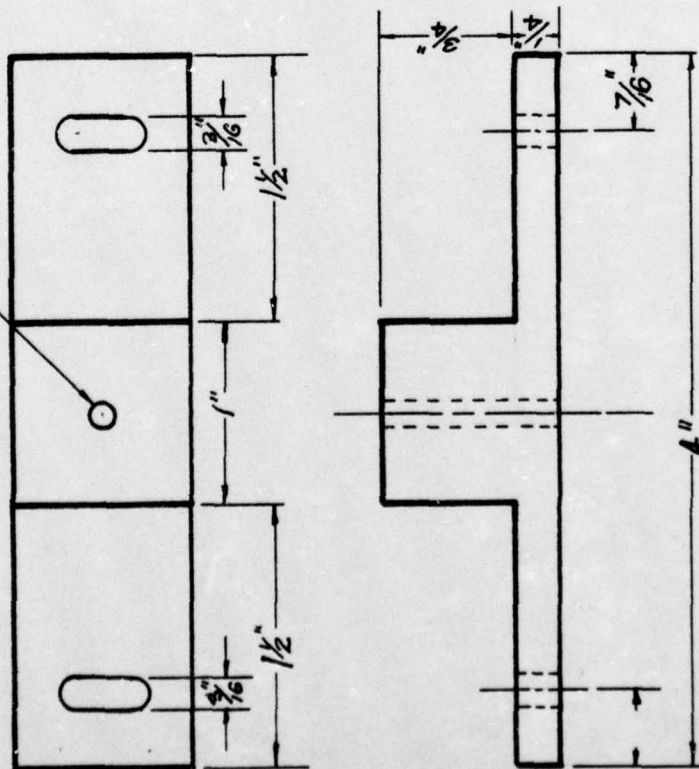
\* NOTE: THE 30mm BORE  
DIMENSION SHOULD  
ALLOW SLIDE FIT OF  
DOUBLE CONVEX LENS

P/N 18  
RETAINER, LENS, 30mm  
MAT'L: ALUMINUM  
DRAWN BY: LT DIMMOSEY  
30 JULY 1976 AHS



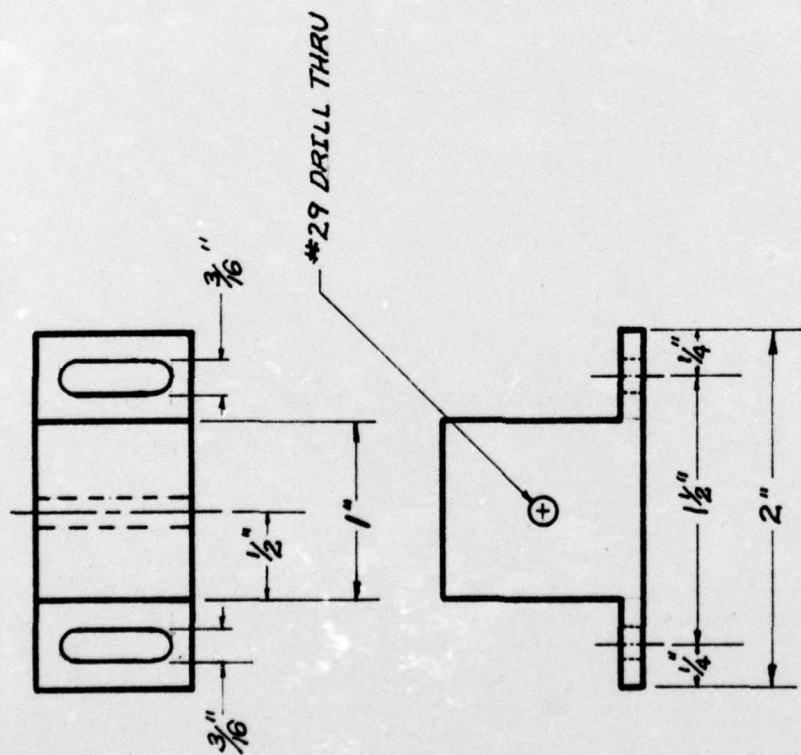
BLA  
PAO

#29 DRILL THRU



P/W 19

MOUNT, FIBER OPTIC, TOP  
 MATERIAL: ALUMINUM  
 DRAWN BY: LT. D. M. MOSEY  
 8 APRIL 1976 NPS



2 REQUIRED

P/N 20

MOUNT, FIBRE OPTIC, END

MATERIAL: ALUMINUM

DRAWN BY: LT. D.M. MOSEY

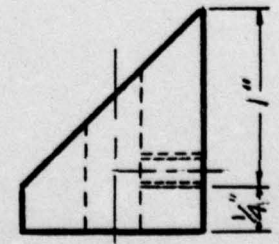
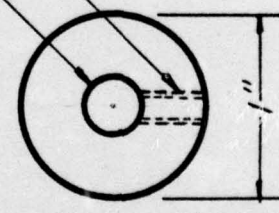
8 APRIL 1976

NPS



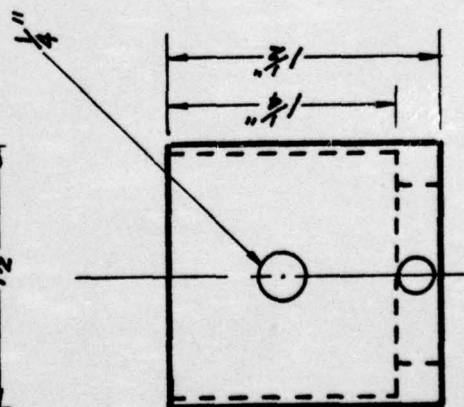
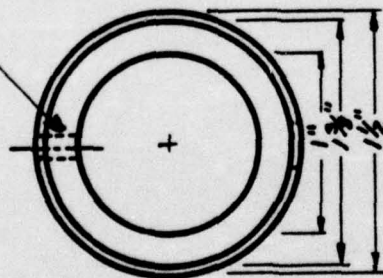
5" THRU HOLE TO MATCH SHAFT

DRILL 1/4" TAP FOR 10-32 SET SCREW

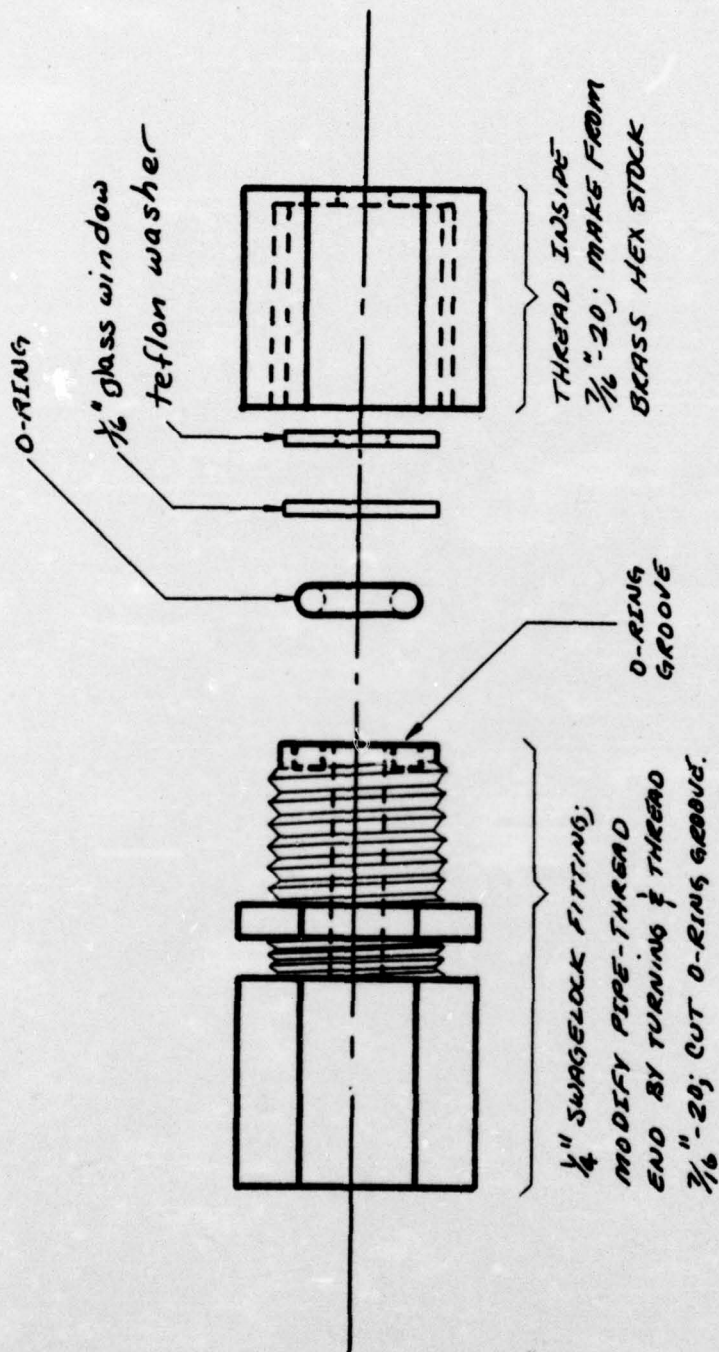


MOUNT, MIRROR P/N 21  
MATERIAL: ALUMINUM  
DRAWN BY: LT. D.M. MOSEY  
2 AUGUST 1976 NPS

DRILL  $\frac{1}{8}$ " TAP 10-32



SHIELD, MIRROR P/N 22  
 MATERIAL: ALUMINUM  
 DRAWN BY: LT. D.M. MOSEY  
 9 SEPT 1976 NPS



TERMINATION DETAIL; P/N 23  
SCATTERING FIBERS  
DRAWN BY: LT D.M. MOSEY  
13 SEPT 1976 NPS



## APPENDIX B

### LIST OF OFF-THE-SHELF COMPONENTS UTILIZED IN THE NPS TRANSMISSOMETER-NEPHELOMETER

1. Motor: 24 VDC, 42 RPM D.C. motor, Magnatorc, Hansen Mfg. Co., Inc., Princeton, Indiana.
2. Gears: 50 tooth, 2 3/16" O.D.
3. Lens: aspheric condenser, unsymmetrical; S/N 40339, Dia. 72.5 mm, F.L. 46 mm; Edmund Scientific Co., Barrington, N. J. 08007 (2 required).
4. Lens: achromat, coated; S/N 6246, Dia. 39 mm, F.L. 63 mm; Edmund Scientific.
5. Lens: achromat, Dia. 30 mm, F.L. 55 mm; Edmund Scientific.
6. Fiber optics; 12 feet required; No. OP736-C, 0.152", 6 foot lengths of jacketed fiber, contains 37 0.017" plastic fibers, 0.119" I.D./0.152" O.D.; International Rectifier Corporation.
7. Terminations: Indicator light for fiber optics; S/N 41232; Edmund Scientific.
8. Glass windows: 3/4" thick Pyrex, 4" Dia.; (2 required).
9. Fittings: Swagelock, 1/4", stainless steel.
10. Bearings: Fafnir F5, (2 required).
11. Lamp: General Electric miniature lamp, #1974, 20W, 6 volt.

12. Detector: PIN-10 solid state photoconductor, P/N 2023;  
United Detector Technology, Santa Monica, California.
13. Waterproof connector: Mecca, #2047 w/o-ring; MECCA,  
P.O. Box 3693, 519 Jessamine, Houston, Texas 77036.
14. O-rings: (for pyrex windows), Parker 2-239 O-ring,  
(2 required).

# BIBLIOGRAPHY

1. Duntley, S. Q., Underwater Lighting by Submerged Lasers and Incandescent Sources, S.I.O. Ref 21-1, pp. 2-1 through 2-26, June 1971.
2. Gilbert, G., Underwater Light Attenuation Data Taken Near San Clemente Island, Naval Weapons Center, China Lake, CA; pp. 1-13, April 1968.
3. Jerlov, N. G. and E. S. Nielsen, Optical Aspects of Oceanography, Academic Press, London and New York, pp. 28-49, 1974.
4. Nichols, D. A., Block 50 Compilation, Defense Meteorological Satellite Program (DMSP), Headquarters Space and Missile Systems Organization, Air Force Systems Command, United States Air Force, pp. 44 and 45, July 1975.
5. Underwater Imaging System Design, Ocean Technology Department, Naval Undersea Center, pp. 2-3 through 2-22, July 1972.



# INITIAL DISTRIBUTION LIST

	No. Copies
1. Department of Oceanography, Code 68 Naval Postgraduate School Monterey, California 93940	3
2. Oceanographer of the Navy Hoffman Building No. 2 200 Stovall Street Alexandria, Virginia 22332	1
3. Office of Naval Research Code 480 Arlington, Virginia 22217	1
4. Dr. Robert E. Stevenson Scientific Liaison Office, ONR Scripps Institution of Oceanography La Jolla, California 92037	1
5. Library, Code 3330 Naval Oceanographic Office Washington, D. C. 20373	1
6. SIO Library University of California, San Diego P. O. Box 2367 La Jolla, California 92037	1
7. Department of Oceanography Library University of Washington Seattle, Washington 98105	1
8. Department of Oceanography Library Oregon State University Corvallis, Oregon 97331	1
9. Commanding Officer Fleet Numerical Weather Central Monterey, California 93940	1
10. Commanding Officer Navy Environmental Prediction Research Facility Monterey, California 93940	1

- |     |   |   |
|-----|---|---|
| 11. | Department of the Navy<br>Commander Oceanographic System Pacific<br>Box 1390<br>FPO San Francisco 96610 | 1 |
| 12. | Defense Documentation Center<br>Cameron Station<br>Alexandria, Virginia 22314                           | 2 |
| 13. | Library (Code 0142)<br>Naval Postgraduate School<br>Monterey, California 93940                          | 2 |
| 14. | Stevens R. Tucker, Code 68Tx<br>Naval Postgraduate School<br>Monterey, California 93940                 | 6 |
| 15. | LT. David M. Mosey USN<br>SWOSCOLCOM<br>Class No. 54<br>Newport, Rhode Island 30465.                    | 2 |